THE THERMAL HISTORY OF THE WESTERN IRISH ONSHORE

Nathan Cogné[1]*, David Chew[1] and Finlay M. Stuart[2]

[1]Department of Geology, Trinity College Dublin, College Green, Dublin 2, Ireland.

[2] SUERC, Rankine Avenue, Scottish Enterprise Technology Park, East Kilbride G75 0QF, United Kingdom.

* Corresponding Author: cognen@tcd.ie

Abstract

We present here a low-temperature thermochronological study that combines the apatite fission track and (U+Th)/He dating methods with a pseudo-vertical sampling approach to generate continuous and well-constrained temperature-time histories from the onshore Irish Atlantic margin. The apatite fission track and (U+Th)/He ages range from the Late Jurassic to Early Cretaceous and the mean track lengths are relatively short. Thermal histories derived from inverse modelling shows that following post-orogenic exhumation the sample profiles cooled to ~75°C. A rapid cooling event to surface temperatures occurred during the Late Jurassic to Early Cretaceous and was diachronous from north to south. It was most likely caused by ~2.5 km of rift-shoulder related exhumation and can be temporally linked to the main stage of Mesozoic rifting in the offshore basins. A slow phase of reheating during the Late Cretaceous and Early Cenozoic is attributed to the deposition of a thick sedimentary sequence that resulted in ~1.5 km of burial. Our data imply a final pulse of exhumation in Neogene times, probably related to compression of the margin. However, it is possible that an Early Cenozoic cooling

event, compatible with our data but not seen in our inverse models, accounts for part of the Cenozoic exhumation.

Supplementary material: Apatite fission track and (U+Th)/He methodologies are available at www.geolsoc.org.uk/

Historically, the almost complete absence of post-Variscan sediments outside of northeastern Ireland has made it difficult to assess the Mesozoic and Cenozoic evolution of onshore Ireland. In contrast, offshore Ireland and Britain make a superb natural laboratory in which to evaluate the various techniques for estimating the timing and magnitude of exhumation because of the wealth of data provided by the hydrocarbon industry (e.g. Corcoran & Doré 2005), such as apatite fission track, vitrinite reflectance and shale compaction data. Therefore the evolution of the surrounding offshore basins has often been used as a proxy to infer the post-Variscan history of the Irish onshore (e.g. Naylor 1992). However without well-established links between the onshore exhumation history and the evolution of the offshore basin fill, such methods cannot be directly used to infer the post-Variscan history of the onshore portion of the Irish Atlantic margin.

The thermal evolution of the Irish landmass has been investigated by extensive thermal maturation studies (e.g. vitrinite reflectance and conodont alteration data) of the Carboniferous and Devonian rocks that cover much of onshore Ireland (Clayton et al. 1989, Goodhue and Clayton 1999). These studies require several kilometres of burial and exhumation to reach their present-day exposure level. Because post-Carboniferous rocks on the Irish mainland do not yield high maturation values, peak maturation temperatures and the majority of the subsequent

exhumation has been attributed to the Variscan orogeny and its unroofing. However many of the details of the subsequent post-Variscan thermal history remained unresolved.

The apatite fission track (AFT) technique has been used during the past two decades to determine more precisely the post-Variscan thermal history of onshore Ireland (e.g. McCulloch 1993, 1994; Kelley et al. 1993; Green et al. 2000; Allen et al. 2002), as low-temperature thermochronological techniques have the advantage of yielding temporally controlled thermal history information (e.g. Gallagher et al. 1998). Green et al. (2000) and McCulloch (1993) have shown that the thermal history of western Ireland is characterised by cycles of exhumation (with subsequent re-burial) during the Mid-Jurassic, Early Cretaceous and Early Cenozoic followed by final exhumation in the Neogene. This Cenozoic thermal history is in broad agreement with the pattern of Cenozoic exhumation on a larger scale (e.g. Ireland and Britain, Hillis et al. 2008). Allen et al. (2002) in contrast argued for more a continuous and progressive Mesozoic to Cenozoic exhumation history, with a phase of reburial restricted to the Late Cretaceous that was then followed by rapid exhumation during the Cenozoic. Therefore aspects of the post-Variscan exhumation history of the Irish onshore remains controversial despite a fairly large database of apatite fission track data.

Consequently in this study we also employ the apatite (U+Th)/He (AHe) thermochronometer in conjunction with the AFT method with the aim of producing better resolved thermal histories. Moreover we also employed a pseudo-vertical profile approach (i.e. summit-to-valley sample transects) on selected targets along the western Irish coast. The thermal history of each profile is characterised by integrating these two thermochronometers to generate better constrained continuous

temperature-time histories than previous thermal history studies from the Irish onshore. Combining data from different samples using a vertical profile approach reduces the uncertainties on the final thermal history model (Gallagher et al. 2005).

Geological setting

Onshore Ireland

Most of central and mid-western Ireland is characterised by relatively flat and subdued topography and is mainly composed of Late Devonian to Carboniferous sedimentary rocks. In contrast, the western Irish Atlantic coastline exhibits comparatively high relief with summits that range from over 750 m in Donegal in the northwest to over 1000 m in Kerry in the southwest. These high elevation regions are typically formed of older rocks, ranging in age from Precambrian to Devonian (Figs. 1 and 2).

Post-Carboniferous outcrops are scarce in western Ireland. In southwest Ireland, the oldest is the Mid-Jurassic (~180 Ma) Cloyne clay (Fig. 1, Higgs and Beese 1986). Vitrinite reflectance values of ~0.35 R_O% (Clayton, 1989) show that the Cloyne clay has undergone approximately 1 km of burial. The Ballydeenlea Chalk (Fig. 1) has featured prominently in many studies of the post-Carboniferous evolution of Ireland (e.g. Dewey 2000; Green et al. 2000; Allen et al. 2002). It is dated as Campanian in age (Barr 1966), which corresponds to an age range of 83.6-72.1 Ma (all stratigraphic ages quoted in this study use the timescale of Gradstein et al., 2012). This outcrop is of particular interest because vitrinite reflectance data (Evans and Clayton 1998) demonstrates that the Ballydeenlea Chalk was buried and heated

to temperatures of 60 - 80°C (0.46 – 0.53 R_O%). In northwest Ireland the aureoles of Palaeocene (62-58 Ma) dyke swarms (Thompson 1985) have yielded AHe ages that are indistinguishable from the intrusion ages of the dykes implying relatively low amounts (<1.5 km) of Cenozoic exhumation in this region (Bennett 2006). Cenozoic sediments locally infill karstified Carboniferous limestones in central Ireland. The oldest examples are Oligocene in age (Fig. 1, Ballygiblin, Simms and Boutler 2000; Ballymacadam, Watts, 1957) but most them are either undated or are Miocene to Pliocene in age (Coxon and McCarron 2009). The preservation of such deposits clearly indicates locally low amounts of Neogene denudation in central Ireland. Based on topographic and fluvial studies, Dewey (2000) argued for fragmented Cenozoic uplift of western Ireland associated with Eocene-Oligocene extensional normal faulting and Miocene to recent compression, with little denudation of the Irish Midlands during the Mesozoic and Cenozoic.

The western Irish offshore basins

On the western Irish margin, proto-Atlantic rifting is characterized by a series of discrete extensional episodes during the Permo-Triassic, Middle to Late Jurassic and Early Cretaceous (Naylor and Shannon 2005) that led to the formation of the western Irish offshore basins (Fig. 2). The Middle to Late Jurassic rifting event is the most significant (Naylor and Shannon 2009). It was diachronous, commencing in the Middle Jurassic in the Slyne and Erris basins (Dancer et al. 1999; Chapman et al. 1999), in the Late Jurassic to Early Cretaceous in the Porcupine Basin (Moore 1992; Shannon et al. 1999; Naylor and Shannon 2005) and in the Early Cretaceous in the Goban Spur Basin (Masson et al. 1984; Naylor and Shannon 2005).

During the Cretaceous and Cenozoic, the evolution of the western Irish offshore basins mainly reflects the effects of thermal subsidence (Shannon 1991; Shannon et al. 1993; McDonnell and Shannon 2001). However each basin experienced different tectonic histories that accounts for their main tectonostratigaphic differences. Phases of local rifting are inferred in the Erris (Chapman et al. 1999) and Porcupine (Naylor and Shannon 2005) basins during Aptian – Albian times (126.3-100.5 Ma). More widespread uplift, possibly related to the effects of the proto-Iceland plume are also recognised in the Porcupine Basin at the Palaeocene-Eocene boundary (e.g. Jones et al. 2001; McDonnell and Shannon 2001). Uplift of the Porcupine High during Palaeogene times has been inferred to have caused an influx of clastic sediments into the Porcupine and Rockall basins (McDonnell and Shannon 2001). Finally uplift related to either Alpine compression and/or Atlantic ridge push has been inferred in the Erris, Slyne and Porcupine basins since the Miocene (Chapman et al. 1999; Dancer et al. 1999; McDonnell and Shannon 2001).

Thermochronology

Sampling strategy

The sampling profiles were selected along the western coast of Ireland so as to detect any north-south variation in the thermal evolution along the Irish Atlantic margin. We sampled four pseudo-vertical profiles, two in County Kerry (Carrauntoohill in Macgillycuddy's Reeks on the Iveragh Peninsula and Mount Brandon on the Dingle Peninsula), Mweelrea in County Mayo and Slieve Snaght in

County Donegal (Figs 1,2). Vertical sample spacing along each profile was 100 m, but not every sample yielded sufficient apatite for analysis. In addition one sample was selected from a clast of Namurian sandstone enclosed in the chalk matrix of the Campanian Ballydeenlea Fm. (Fig. 1).

.

Fission track analyses

The detailed apatite fission track methodology is provided in the supplementary material. All samples were prepared and analysed in Trinity College Dublin (TCD). The etching protocol was very similar to the procedures described by Donelick et al. (2005). Uranium concentration measurements for fission track dating were measured by LA-ICPMS at TCD following the protocols described in Donelick et al. (2005) and. Chew and Donelick (2012). Apatite Cl concentration measurements (Chew et al. 2014a) and apatite U-Pb age data (Chew et al. 2014b) were also obtained from the same LA-ICPMS spot ablations.

(U+Th)/He

A full description of the (U+Th)/He methodology is provided in the supplementary material. All apatite grains were picked in TCD and all (U+Th)/He measurements were carried out at the Scottish Universities Environmental Research Center (SUERC). All procedures are described in detail in Foeken et al. (2006). The minimum uncertainty on the calculated ages of the apatite unknowns is fixed at 10% based on repeated (U+Th)/He measurements of the Durango apatite standard.

Results

The AFT ages range from 131.8 ± 11.0 Ma to 200.1 ± 17.8 Ma (2•; Table 1). The mean track length (MTL) is similar in all profiles, ranging from 11.8 ± 0.19 μm to 12.9 ± 0.19 μm (1 SE) with standard deviations of between 1.87 μm and 2.33 μm. The chlorine content of the samples measured by ICPMS ranges from 0.02 to 0.15 wt%, indicating that the analysed grains are fluoroapatites that are similar to Durango apatite in terms of their annealing characteristics. The kinetic parameter ,$D_{par,}$, ranges from 1.3 to 2.08 μm, similar to Durango apatite (mean D_{par} measured for the same etching protocol is 1.66 μm). Overall these results for the apatite unknowns are in good accordance with previously published fission track work from the Irish mainland (Fig. 3a).

All but one sample passed the χ^2 test (Galbraith 1981, modified by Donelick et al. 2005 for LA-ICPMS fission track data) and the single grain age distributions are unimodal. A plot of AFT age *vs* MTL shows a slight decrease in MTL with increasing age, although this correlation is mainly due to the Slieve Snaght profile that yields older ages and lower MTLs compared to the other profiles (Fig. 3a).

There is no clear correlation between AFT age and elevation (Fig. 3b), but the youngest ages for each sample in our dataset typically come from low elevations. Similarly it seems that the ages are slightly younger towards south, although this trend is not statistically significant at the 2σ level.

AHe ages range from 78.2 ± 7.8 Ma to 216.5 ± 21.6 Ma (1σ, uncorrected) and from 96.4 ± 9.6 Ma to 267.9 ± 26.8 Ma (1σ, F_T-corrected) (Table 2). Some of the aliquots exhibit older F_T-corrected ages than the corresponding AFT age (Fig. 4a). However, numerous authors (e.g. Green et al. 2006 and Shuster and Farley 2009)

have shown that the amount of α-recoil damage has a strong influence on the effective closure temperature of the AHe system. This amount of damage can be approximated by the effective uranium (eU) factor where eU = [U] + 0.24 [Th] (Green et al., 2006). In our dataset eU and AHe age are only weakly correlated, although most of the He aliquots that are older than the corresponding AFT age have relatively high eU values (Fig. 4a and 4b). The AHe ages tend to be younger towards the bottom of each profile, but there is not a clear correlation between AHe age and elevation (Table 2). As observed in the AFT ages, AHe ages are slightly younger in the south than in the north (Table 2, Fig. 4b).

Interpretation

The Late Jurassic and Early Cretaceous fission track ages and the relatively short MTLs obtained in this study are similar to previously published AFT data from the Irish mainland (McCulloch 1993, Green et al. 2000; Allen et al. 2002). In general, both the AFT and AHe ages for each sample are younger than the depositional (or crystallization) ages with the exception of the Ballydeenlea sample. This is expected as the Devonian and Ordovician clastic sedimentary rocks have undergone low-grade metamorphism at temperatures significantly higher than the PAZ. Moreover both the AFT and AHe methods yield similar ages from the same samples for the Jurassic to Early Cretaceous. Therefore it seems likely that our data record an important thermal event during this time period.

Inverse modelling methodology

226 Inverse modelling of the AHe and AFT (track length and age) data from the
227 pseudo-vertical profiles has been undertaken to extract thermal history information.
228 We used the QTQt software. QTQt employs a Bayesian trans-dimensional Markov
229 Chain Monte Carlo (MCMC) approach (Sambridge et al. 2006; Gallagher et al. 2009).
230 The modelling procedure is fully described in Gallagher (2012).
231 In this study a general time-temperature box (75±75°C, variable in time
232 according to the oldest observed age) is used as the parameter space. A series of
233 discrete time-temperature points are sampled from this to construct a continuous
234 thermal history and the data likelihood is calculated for that model. To model the
235 fission track data, we used the individual track counts, measurements of confined
236 length and angle to c-axis, the likelihood function of Gallagher (1995) and the
237 annealing model of Ketcham et al. (2007). The measured AHe ages were modelled
238 using a spherical diffusion formulation, simulating both alpha-ejection and diffusion
239 during the thermal history (Meesters and Dunai 2002) combined with the radiation
240 damage model of Flowers et al. (2009).
241 The present-day temperature for the top sample of each profile is set at 5 ± 5
242 °C and a present-day offset between the top and bottom sample is set at 10 ± 5 °C.
243 We also used independent geological evidence for the high-temperature start point
244 on each profile, such as the timing of low-grade metamorphism or the U-Pb apatite
245 age as determined by LA-ICPMS. Finally the Late Cretaceous depositional age of the
246 Ballydeenlea sample also provides another constraint on its thermal history
247 modelling. All models employed 200,000 iterations which is sufficient to provide
248 stable solutions (Gallagher 2012).
249 In the following section we consider the weighted mean model (termed the
250 expected model), while credible intervals (the Bayesian equivalent of confidence

intervals) were calculated using the ensemble of thermal history solutions. These credible intervals then represent the range of the model parameters contained in the posterior distribution at the specified level of probability (e.g. 95%).

Inverse modelling results

The expected thermal history model for each profile is depicted in Fig. 5 and the associated predicted AFT-AHe ages and MTLs are illustrated in Figs. 6 and 7 respectively. The next section describes the thermal history trends observed on each profile from north to south. The temperatures reported are for the coolest (i.e. highest elevation) sample from each profile.

Slieve Snaght (Fig. 5a): Although the Main Donegal Granite has yielded a 407±4 Ma crystallization age (O'Connor et al. 1984), the LA-ICPMS U-Pb apatite data suggest that the batholith remained at temperatures of c. 450°C (the typical closure temperature of the U-Pb apatite system; Chamberlain and Bowring 2001) until 384.0±2.9 Ma and this is adopted as the high temperature constraint in this study. At ~365 Ma the granite was already in the PAZ and remained at ~75°C until 180 Ma when it underwent 50°C of cooling over 30 Ma. The rock was then reheated from surface temperatures to ~55°C at 15 Ma followed by a final cooling event that exhumed the samples to the surface.

Mweelrea (Fig. 5b): Low-grade Caledonian deformation of the Mweelrea succession is locally constrained to post-Darriwilian, pre-Telychian times (i.e. 458.4-438.5 Ma). The peak temperature of low-grade Caledonian deformation is not known exactly and so a temperature range of 200±50°C was employed. The rocks then cooled to around 45°C by 380 Ma, before undergoing slow reheating to re-enter the

PAZ and reaching ~80°C by 250 Ma. An episode of slow cooling then began and the samples reached ~75°C at 155 Ma. Rapid Late Jurassic-Early Cretaceous cooling (155-125 Ma) at ~2°C/Myr brought the samples to surface temperatures. As with the Slieve Snaght profile, the rocks then underwent reheating to reach 50°C by 10 Ma before they were exhumed to the surface.

Mount Brandon (Fig. 5c): Following Variscan metamorphism the samples cooled rapidly to ~70 °C by 270 Ma. They then remained at stable temperatures until 150 Ma, when a cooling episode of 25 Ma duration brought the rocks to surface temperatures. A reheating event of about 35°C occurred until 20 Ma before final cooling to surface temperatures.

Carrauntoohill (Fig. 5e): As with the Mount Brandon profile, the Carrauntoohill samples reached the PAZ at around 275 Ma. Notably in both profiles the peak temperatures associated with Variscan metamorphism were insufficient to reset the U-Pb apatite system which are dominated by detrital apatite U-Pb ages of c. 420 Ma. Following Variscan metamorphism the samples then cooled very slowly (<0.1 °C/Ma), reaching 70 °C at 125 Ma. A fast cooling episode then brought the samples to surface temperatures by 100 Ma. Following this episode there was a long phase of slow reheating until 12 Ma before a final cooling event of about 35°C to surface temperatures.

Ballydeenlea sample (Fig. 5d): This sample exhibits a similar thermal history to the Mount Brandon profile. However the apatite in this sample is taken from a clast of Namurian (ca. 329-318 Ma) sandstone that was incorporated into the Ballydeenlea Chalk during the Campanian (83.6-72.1 Ma). The pre-Campanian history is therefore inherited from the Namurian source. It records a cooling episode of 60°C between 150 Ma and 125 Ma, and the sample remained close to surface temperatures until it

was incorporated into the Ballydeenlea Chalk at ~75 Ma. The Ballydeenlea Chalk then underwent reheating to 55°C at 20 Ma before a final late cooling event brought it back to the surface.

The thermal history models of the profiles indicate that the samples cooled rapidly into the PAZ following the early high temperature constraint(s). Temperatures then remained more or less stable (given the uncertainty on the thermal histories) until a period of rapid cooling during the Mesozoic. This cooling episode occurred during the Mid-Late Jurassic for the northern profile (180-150 Ma for Slieve Snaght), during the Late Jurassic to Early Cretaceous for the Mweelrea profile (155-125 Ma) and for Mount Brandon (150-120 Ma) and during the Early Cretaceous for the southern Carrauntoohill profile (125-100 Ma). The pre-Campanian history of the Ballydeenlea sample is inherited from its source region (although this source region is likely to have been very proximal to the Ballydeenlea Chalk deposit) and shows Early Cretaceous cooling similar to the Mount Brandon profile. This Mesozoic cooling episode is the most striking feature of our models. Following this phase of rapid cooling, a phase of slow reheating is inferred to have occurred until Neogene times before a final phase of cooling to surface temperatures.

Discussion

Pre-rift history

The data for all profiles indicate a phase of rapid cooling following the last significant high-temperature pulse. In the northern profiles, this rapid cooling is associated with the post-Caledonian exhumation whereas in the southern profiles

326 rapid post-Variscan exhumation is apparent. With the exception of the Mweelrea
327 profile it appears that the samples then remained at relatively stable temperatures
328 until Jurassic or Cretaceous times. For the Mweelrea profile, post-Caledonian
329 exhumation to near surface temperatures at 380 Ma was followed by a reheating
330 phase from 340 Ma until 250 Ma. This is in good agreement with the occurrence of
331 Tournaisian (358.9-346.7 Ma) sedimentary rocks that unconformably overlie the
332 Mweelrea Formation at an elevation of greater than 600 m on the plateau surface
333 less than 15 km east of Mweelrea summit. Thus, despite the large uncertainties on
334 this portion of the thermal history, it seems likely that a relatively thick (~1 to 2 km)
335 sequence of Carboniferous sedimentary rocks was deposited in this region following
336 Late Caledonian exhumation.
337
338 *Mid-Jurassic – Early Cretaceous cooling phase*
339
340 Previous thermochronological studies in Ireland have yielded somewhat
341 contradictory Mesozoic thermal histories. Allen et al. (2002) argued for a prolonged
342 period of low denudation during the Mesozoic, while Green et al. (2000) proposed
343 that the Irish mainland underwent at least two cycles of exhumation and subsequent
344 reburial during the Mid-Jurassic and Early Cretaceous. Similarly Holford et al. (2010)
345 proposed multiple phases of exhumation in Scotland during the Jurassic and Early
346 Cretaceous while Holford et al. (2009) working in the Irish Sea area proposed one
347 main Mesozoic phase of exhumation during the Early Cretaceous. In both these latter
348 studies, Early Cretaceous exhumation was attributed to the onset of sea-floor
349 spreading which initiated SW of Ireland at around 125 Ma.

An important Mesozoic cooling phase is recorded by our dataset. This cooling phase is diachronous along western Ireland, beginning close to the Lower-Mid Jurassic boundary (180 Ma) for the Slieve Snaght profile, during the Late Jurassic (155 Ma) for Mweelrea, close to the Jurassic-Cretaceous (150 Ma) boundary for Mount Brandon and Ballydeenlea and during the Upper Cretaceous (125 Ma) for Carrauntoohill. Therefore on the scale of Western Ireland our results are broadly similar to those Green et al. (2000). However instead of interpreting our results as evidence for multiple exhumation episodes, we argue here for one cooling phase that becomes younger towards the south. While migration of the Irish margin above dynamic topography could explain such an age pattern, there is no evidence in the Western Irish offshore for an active plume during rifting as there is in the North Sea (e.g. Underhill and Partington 1993). Additionally, this migration of the locus of cooling is not observed elsewhere in Ireland and Britain. The cooling phase is also older than the cooling phases inferred by Holford et al. (2009) and precedes the onset of sea-floor spreading. Thus we propose here that the observed cooling in Western Ireland is linked to rift shoulder uplift and erosion associated with the slow propagation southwards of mid-Mesozoic rifting along the Western Irish margin.

Several episodes of rifting took place along the Irish Atlantic margin from the Permo-Triassic to the Upper Cretaceous (e.g Naylor and Shannon 2005). The timing of the most significant Mesozoic rifting event appears diachronous along the margin as it took place in the Mid-Jurassic in the Erris and Slyne basins (Dancer et al. 1999; Chapman et al. 1999) whereas it is constrained to the Late Jurassic to Early Cretaceous in the Porcupine Basin (Moore 1992; Shannon et al., 1999; Naylor and Shannon 2005). The onset of cooling as inferred from the inverse modelling of the Slieve Snaght, Mweelrea and Mount Brandon profiles and for the Namurian source

region of the Ballydeenlea sample is therefore in good agreement with the timing of rifting in the offshore basins. The Carrauntoohill profile indicates a younger onset of cooling compared to the main phase of rifting in the Porcupine Basin directly to the west. However Aptian-Albian (126.3-100.5 Ma) deltaic sandstones are reported in the Porcupine Basin that were deposited during a local episode of rifting (Naylor and Shannon 2005), while the initiation of rifting in the Goban Spur Basin (southwest of the Inveragh peninsula, Fig. 2) is Hauterivian (133.9-130.8 Ma) (Naylor and Shannon 2005) or Barremian (130.8-126.3 Ma) (Masson et al., 1984) in age. It therefore appears likely that our southern profile is influenced by this late stage of rifting on the southwest portion of the Irish Atlantic margin.

It should be noted that whereas our data indicate only one significant Mesozoic cooling phase, there is often evidence for more than one phase of Mesozoic rifting in the western Irish offshore basins (e.g. Naylor and Shannon 2005). The sensitivity of the low-temperature thermochronological techniques employed means that they cannot record discrete exhumation episodes that are close together in time. Therefore the inverse modelling approach adopted here records the total amount of cooling but only temporally discriminates the most significant cooling phase.

This cooling episode typically lasts for 25 to 30 Ma and the total amount of cooling is ~50°C. The amount of exhumation can be estimated by assuming a palaeogeothermal gradient. The pseudo-vertical profile approach adopted here shows that the temperature offset between the coolest and the hottest sample from the same profile did not exceed 18°C (for a maximum elevation offset of about 900 m), implying the palaeogeothermal gradient did not exceed 20°C/km. Although this is a relatively low value for a rift setting it is not unreasonable (e.g. Seiler et al. 2011). It

400 is also in agreement with the present-day geothermal gradient in western Ireland
401 (Goodman et al. 2004). A cooling phase of 50°C therefore implies around 2.5 km of
402 exhumation and thus Mesozoic rift-shoulder exhumation is an important feature of
403 the evolution of the onshore Irish Atlantic margin.
404
405 *The post-rift history*
406
407 Inverse modelling of our dataset shows that following Mesozoic rift-related
408 cooling and exhumation the region underwent reheating until the Neogene. This is
409 indicated by the track length distribution of our samples that show relatively short
410 MTLs (11.8-12.9 μm), which clearly indicates that the samples cannot have resided
411 at surface temperatures since the Mesozoic. In our models, the 30-35°C heating
412 event that followed Mesozoic rifting corresponds to burial depths of about 1.5 km.
413 However it should be noted that the exact timing of both the heating and
414 cooling episodes during the Late Cretaceous and Cenozoic is not well constrained.
415 Our thermal history models indicate a simple cycle of slow heating and rapid late
416 (Neogene) cooling. However the software used in this study for the inverse modelling
417 uses a Bayesian approach that tends to favour the simplest thermal history models
418 (Gallagher, 2012). Additionally the thermochronological techniques employed are not
419 sensitive at the low temperatures (20-40°C) inferred during the Late Cretaceous and
420 for a large part of the Cenozoic. It is therefore possible that the thermal history that
421 followed Mesozoic rift-flank exhumation is more complex than that depicted. Forward
422 modelling cannot easily discriminate between different possible Cenozoic thermal
423 histories at such low temperatures, and so even though the thermal histories are well
424 constrained due to modelling a combination of AFT and AHe data from pseudo-

425 vertical profiles, the exact timing of burial and exhumation during the Late
426 Cretaceous-Cenozoic remains uncertain.

427 Previous thermochronological studies (Green et al. 2000 and Allen et al. 2002)
428 have argued for Late Cretaceous transgression and chalk deposition on the Irish
429 mainland. This is in agreement with the inferred 1.5 km burial derived from the
430 thermal history modelling of the profiles and the Ballydeenlea Chalk sample in this
431 study, along with existing vitrinite reflectance data from the Ballydeenlea Chalk (post-
432 Campanian burial temperatures of ~60-80°C; Evans and Clayton 1998). To produce
433 ~1.5 km of burial under marine sedimentary rocks we need to assume that the
434 topography inherited from Mesozoic rift-shoulder uplift was subsequently eroded
435 away. The Mesozoic cooling episode of ~30 Ma duration is in agreement with this
436 scenario, as it allows enough time to erode the rift topography (e.g. Brown et al.
437 2002; Flowers and Schoene 2010; Japsen et al. 2011). It is also thought likely that
438 during the Campanian deposition of the Ballydeenlea Chalk a large part of Ireland,
439 and not only the western margin, was below sea level (Evans and Clayton 1998;
440 Dewey 2000; Naylor 1998). Late Cretaceous chalk deposition thus provides a good
441 candidate burial mechanism but the timing of the initiation of Late Cretaceous
442 sedimentation and the duration of burial is not well known. The difference in vitrinite
443 reflectance values between the Mid Jurassic Cloyne Clay (0.35 R_O%) and the
444 Campanian Ballydeenlea Chalk (0.46 – 0.53 R_O%) show that the thickness of the
445 sedimentary cover was variable and suggests it may have been thicker towards the
446 west.

447 Similarly determining the timing of the onset of Cenozoic exhumation is
448 problematic due to the lack of sensitivity of the thermochronometers at near-surface
449 temperatures. Several authors have suggested that Ireland underwent Early

450 Cenozoic reactivation and exhumation based on both thermochronological data
451 (Allen et al. 2002; Green et al. 2000) and also structural evidence (Dewey 2000).
452 Regional tectonostratigraphic studies (e.g. Brodie and White 1994; White and Lovell
453 1997; Jones et al. 2002) have argued that Early Cenozoic exhumation related to the
454 proto-Iceland plume is widespread on this segment of the NW European margin (i.e.
455 throughout much of Britain and Ireland). This is backed up by thermochronological
456 data in Scotland (Persano et al. 2007) that has yielded evidence of Early Cenozoic
457 exhumation. However, other studies from the Irish Sea region have argued for more
458 localised inversion and exhumation during the Palaeocene (Holford et al. 2005a, b,
459 Hillis et al. 2008). In parts of northwest Ireland the present exposure level may not
460 have changed significantly (<1.5 km exhumation) since the Early Cenozoic based on
461 AHe ages from the aureoles of Palaeocene dyke swarms (Bennett 2006). The local
462 preservation of Oligocene sediments as karstic infills in central Ireland shows that
463 parts of the island have undergone minimal post-Oligocene denudation, implying a
464 pattern of differential Neogene exhumation between western and central Ireland.

465 To test the ability of our dataset to detect a possible phase of Early Cenozoic
466 cooling in western Ireland we added two constraints ("boxes") to the thermal history
467 models to simulate a phase of more rapid heating during the Cretaceous
468 (constrained at 65±10 Ma and 60±10°C) and a cooling pulse during the Early
469 Cenozoic (constrained at 50±10 Ma and 35±10°C). The results of the inverse
470 modelling using these constraints are shown in Fig. 8 for the Mount Brandon profile.
471 The inverse thermal history models generated using these constraints (and the
472 associated predictions) do not differ significantly from the unconstrained inverse
473 models. The thermal history still shows a significant phase of Late Jurassic to Early
474 Cretaceous cooling. A phase of reheating then occurs to respect the first user-

475 specified constraint and is followed by a cooling pulse of 20°C to respect the second
476 user-specified constraint. The samples then remain at stable temperature until 10 Ma
477 before rapid cooling to surface temperatures took place. Therefore our dataset is
478 unable to discriminate between thermal histories with or without Early Cenozoic
479 cooling, which is not surprising given the low temperatures (30–40°C) at which such
480 a cooling event would have occurred.

481 Our inverse modelling clearly indicates a significant pulse (1.5 km) of late
482 Neogene exhumation to return the samples to the surface. It is unlikely that this
483 Neogene exhumation pulse is an artefact linked to the annealing model as discussed
484 by Dempster and Persano (2006) and Redfield (2010). Firstly, the annealing model of
485 Ketcham et al. (2007) uses a curvilinear form of the annealing equation that should
486 not produce this kind of artefact, or at least significantly reduces it (Ketcham et al.
487 2007; Redfield 2010). Secondly, Green et al. (2000) presented evidence for Neogene
488 cooling from two boreholes samples at depths of 1132 m (Ballyragget borehole,
489 County Kilkenny, central Ireland) and 1707 m (Dowra borehole, County Cavan,
490 northwest Ireland). The Neogene cooling episode is better constrained in these
491 borehole samples as they presently are at greater depths. Finally, Late Neogene
492 onshore exhumation seems to be a common feature of the NW European margin
493 (e.g. Japsen and Chalmers 2000, Stoker et al. 2005, Hillis et al. 2008). Therefore we
494 are confident that the phase of Neogene exhumation on the western Irish onshore
495 inferred from the thermal history models is not a modelling artefact, although it is
496 plausible that a component of the Cenozoic exhumation in western Ireland took place
497 in the Palaeogene.

498 Figure 9 synthesizes evolution of Western Ireland. The origin of the postulated
499 pulse of Palaeogene exhumation remains enigmatic, whereas the inferred phase of

Neogene exhumation could likely be explained by the far-field compressional effects of the Alpine orogeny and mid-Atlantic ridge push, as proposed by Hillis et al. (2008) for southern Britain and Ireland. Pleistocene glaciation may have also have been responsible for a small component of the Late Cenozoic exhumation. Importantly the present-day landscape of western Ireland is relatively recent and is not inherited from the Varsican orogenic belt or from Mesozoic rift-related topography.

Conclusion

The use of integrated low-temperature thermochronological techniques (AFT and AHe) combined with a pseudo-vertical sampling approach generates continuous temperature-time histories that are significantly better constrained than models derived from individual samples. The thermal history modelling demonstrates that the western margin of Ireland has experienced a relatively complex thermal evolution during the Mesozoic and Cenozoic. Following post-orogenic cooling and exhumation, the majority of the investigated profiles remained at stable temperatures within the PAZ during the Carboniferous to Early Mesozoic. The most apparent feature of the thermal history models is a significant episode of cooling during the Mid to Late Jurassic in northwest Ireland and during the Late Jurassic to Early Cretaceous in southwest Ireland. About 2.5 km of exhumation took place probably driven by rift shoulder uplift and subsequent erosion. The Late Cretaceous and Cenozoic evolution of the western Irish onshore remains more uncertain as the thermochronological techniques are not sensitive at temperatures < 40°C to small magnitude cooling and/or reheating events. We infer that the sample profiles underwent reheating

525 during the Late Cretaceous to Early Cenozoic that was related to burial beneath ca.
526 1.5 km of sedimentary rocks. This is in agreement with vitrinite reflectance data from
527 the Campanian Ballydeenlea Chalk in southwest Ireland. This cover was removed
528 during the Cenozoic. Our dataset points to a final pulse of exhumation in Neogene
529 times, probably related to compression of the margin and possibly augmented by a
530 phase of enhanced erosion associated with Pleistocene glaciation. However, it is
531 possible that an Early Cenozoic exhumation event, compatible with our data but not
532 seen in our thermal histories derived from the inverse models, accounts for part of
533 the Cenozoic exhumation.
534
535 **Acknowledgments**
536
537 This work has been funded by an Irish Research Council Empower post-
538 doctoral fellowship. Luigia di Nicola is thanked for technical assistance with the
539 apatite (U+Th)/He analyses. Chris Mark is acknowledged for useful discussions that
540 helped improve this manuscript. The careful and insightful reviews of Paul Green
541 and an anonymous reviewer are gratefully acknowledged.
542
543 **References**
544
545 ALLEN, P.A., BENNETT, S.D., CUNNINGHAM, M.J.M., CARTER, A., GALLAGHER, K.,
546 LAZZARETTI, E., GALEWSKY, J., DENSMORE, A.L., PHILLIPS, W.E.A., NAYLOR, D., HACH,
547 C.S., 2002. The post-Variscan thermal and denudational history of Ireland. in: Doré,
548 A.G., Cartwright, M.S., Stoker, M.S., Turner, J.P., White, N. (Eds.), *Exhumation of*
549 *the North Atlantic margin: timing, mechanisms and implications for the petroleum*
550 *exploration. Geological Society, London, Special Publications*, **196**, 371-399.

551 BARR, F.T., 1966. Upper Cretaceous foraminifera from the Ballydeenlea chalk,

552 County Kerry, Ireland. *Paleontology* **9**, 492-510.

553 BENNETT, S.D., 2006. *Tertiary dykes in northwest Ireland: field occurence,*
554 *emplacement mechanisms, host rock deformation, and post-emplacement strain and*
555 *denudations*. Unpublished Ph.D thesis, University of Dublin.

556 BRODIE, J., WHITE, N., 1994. Sedimentary basin inversion caused by igneous
557 underplating: Northwest European continental shelf. *Geology* **22**, 147-150.

558 BROWN, R.W., SUMMERFIELD, M.A., GLEADOW, A.J.W., 2002. Denudational history
559 along a transect across the Drakensberg Escarpment of southern Africa derived from
560 apatite fission track thermochronology. *Journal of Geophysical Research* **107**, 2350.

561 CHAMBERLAIN, K.R., BOWRING, S.A., 2001. Apatite-feldspar U-Pb
562 thermochronometer: a reliable, mid-range (~450°C), diffusion-controlled system.
563 *Chemical Geology* **172**, 173-200.

564 CHEW, D.M., DONELICK, R.A., 2012. Combined apatite fission track and U-Pb
565 dating by LA-ICPMS and its application in apatite provenance analysis. *Mineralogical*
566 *Association of Canada Short Course* **42**, 219-247.

567 CHEW, D.M., SYLVESTER, P.J., TUBRETT, M.N., 2011. U-Pb and Th-Pb dating of
568 apatite by LA-ICPMS. *Chemical Geology* **280**, 200-216.

569 CHEW, D.M., DONELICK, R.A., DONELICK, M.B., KAMBER, B.S., STOCK, M., 2014a
570 Apatite chlorine concentration measurements by LA-ICP-MS. *Geostandards and*
571 *Geoanalytical Research*, **38**, 23-35.

572 CHEW, D.M., PETRUS, J.A., KAMBER, B.S., 2014b. U-Pb LA-ICPMS dating using
573 accessory mineral standards with variable common Pb. *Chemical Geology* **363**, 185-
574 199.

575 CLAYTON, G., 1989. Vitrinite reflectance data from the Kinsale Harbour - Old
576 Head of Kinsale area, southern Ireland, and its bearing on the interpretation of the
577 Munster Basin. *Journal of the Geological Society* **146**, 611-616.

578 CLAYTON, G., HAUGHEY, N., SEVASTOPULO, G.D., BURNETT, R.D., 1989. *Thermal*
579 *maturation levels in the Devonian and Carboniferous of Ireland*. Geological Survey of
580 Ireland ISBN 0951500600.

581 CORCORAN, D.V., DORÉ, A.G., 2005. A review of techniques for the estimation of

582 magnitude and timing of exhumation in offshore basins. *Earth-Science Reviews* **72**,
583 129-168.

584 COXON, P., MCCARRON, S.G., 2009. Cenozoic: Tertiary and Quaternary (until
585 11,700 years before 2000), in: Holland, C.H., Sander, I.S. (Eds.), *The geology of*
586 *Ireland*, 2nd edition. Dunedin Academic Press ltd, Edinburgh, Scotland.

587 DANCER, P.N., ALGAR, S.T., WILSON, I.R., 1999. Structural evolution of the Slyne
588 Trough. *Geological Society, London, Petroleum Geology Conference series* **5**, 445-
589 453.

590 DEMPSTER, T.J., PERSANO, C., 2006. Low-temperature thermochronology:
591 Resolving geotherm shapes or denudation histories? *Geology* **34**, 73-76.

592 DEWEY, J.F., 2000. Cenozoic tectonics of western Ireland. *Proceedings of the*
593 *Geologists' Association* **111**, 291-306.

594 DONELICK, R.A., O'SULLIVAN, P.B., KETCHAM, R.A., 2005. Apatite Fission-Track
595 Analysis. *Reviews in Mineralogy and Geochemistry* **58**, 49-94.

596 EVANS, A., CLAYTON, G., 1998. The geological history of the Ballydeenlea Chalk
597 Breccia, County Kerry, Ireland. *Marine and Petroleum Geology* **15**, 299-307.

598 FLOWERS, R.M., SCHOENE, B., 2010. (U-Th)/He thermochronometry constraints
599 on unroofing of the eastern Kaapvaal craton and significance for uplift of the southern
600 African Plateau. *Geology* **38**, 827-830.

601 FLOWERS, R.M., KETCHAM, R.A., SHUSTER, D.L., FARLEY, K.A., 2009. Apatite (U-
602 Th)/He thermochronometry using a radiation damage accumulation and annealing
603 model. *Geochimica et Cosmochimica Acta* **73**, 2347-2365.

604 FOEKEN, J.P.T., STUART, F.M., DOBSON, K.J., PERSANO, C., VILBERT, D., 2006. A
605 diode laser system for heating minerals for (U-Th)/He chronometry. *Geochemistry,*
606 *Geophysics, and Geosystems* **7**, Q04015.

607 GALBRAITH, R.F., 1981. On statistical models for fission track counts. *Journal of*
608 *the International Association for Mathematical Geology* **13**, 471-478.

609 GALLAGHER, K., 1995. Evolving temperature histories from apatite fission-track
610 data. *Earth and Planetary Science Letters* **136**, 421-435.

611 GALLAGHER, K., 2012. Transdimensional inverse thermal history modeling for

612 quantitative thermochronology. *Journal of Geophysical Research* **117**, B02408.

613 GALLAGHER, K., BROWN, R., JOHNSON, C., 1998. Fission track analysis and its
614 applications to geological problems. *Annual Review of Earth and Planetary Sciences*
615 **26**, 519-572.

616 GALLAGHER, K., STEPHENSON, J., BROWN, R., HOLMES, C., FITZGERALD, P., 2005.
617 Low temperature thermochronology and modeling strategies for multiple samples 1:
618 Vertical profiles. *Earth and Planetary Science Letters* **237**, 193-208.

619 GALLAGHER, K., CHARVIN, K., NIELSEN, S., SAMBRIDGE, M., STEPHENSON, J., 2009.
620 Markov chain Monte Carlo (MCMC) sampling methods to determine optimal models,
621 model resolution and model choice for Earth Science problems. *Marine and*
622 *Petroleum Geology* **26**, 525-535.

623 GOODHUE, R., CLAYTON, G., 1999. Organic maturation levels, thermal history
624 and hydrocarbon source rock potential of the Namurian rocks of the Clare Basin,
625 Ireland. *Marine and Petroleum Geology* **16**, 667-675.

626 GOODMAN, R., G.L., J., KELLY, J., SLOWEY, E., O'NEILL, N., 2004. *Geothermal*
627 *Energy Resource Map of Ireland*. Final Report.

628 GRADSTEIN, F., OGG, J., SCHMITZ, M., OGG, G., 2012. *The Geologic Time Scale*
629 *2012*. Elsevier.

630 GREEN, P.F., DUDDY, I.R., HEGARTY, K.A., BRAY, R.J., SEVASTOPULO, G.,
631 CLAYTON, G., JOHNSTON, D., 2000. The post-Carboniferous evolution of Ireland:
632 evidence from Thermal History Reconstruction. *Proceedings of the Geologists'*
633 *Association* **111**, 307-320.

634 GREEN, P.F., CROWHURST, P.V., DUDDY, I.R., JAPSEN, P., HOLFORD, S.P., 2006.
635 Conflicting (U-Th)/He and fission track ages in apatite: Enhanced He retention, not
636 anomalous annealing behaviour. *Earth and Planetary Science Letters* **250**, 407-427.

637 HIGGS, K., BEESE, A.P., 1986. A Jurassic Microflora from the Colbond Clay of
638 Cloyne, County Cork. *Irish Journal of Earth Sciences* **7**, 99-109.

639 HILLIS, R.R., HOLFORD, S.P., GREEN, P.F., DORÉ, A.G., GATLIFF, R.W., STOKER,
640 M.S., THOMSON, K., TURNER, J.P., UNDERHILL, J.R., WILLIAMS, G.A., 2008. Cenozoic
641 exhumation of the southern British Isles. *Geology* **36**, 371-374.

HOLFORD, S.P., GREEN, P.F., TURNER, J.P., 2005a. Palaeothermal and compaction studies in the Mochras borehole (NW Wales) reveal early Cretaceous and Neogene exhumation and argue against regional Palaeogene uplift in the southern Irish Sea. *Journal of the Geological Society* **162**, 829-840.

HOLFORD, S.P., TURNER, J.P., GREEN, P.F., 2005b. Reconstructing the Mesozoic - Cenozoic exhumation history of the Irish Sea basin system using apatite fission track analysis and vitrinite reflectance data. *Geological Society, London Petroleum Geology Conference series* **6**, 1095-1107.

HOLFORD, S.P., GREEN, P.F., DUDDY, I.R., TURNER, J.P., HILLIS, R.R., STOKER, M.S., 2009. Regional intraplate exhumation episodes related to plate-boundary deformation. *Geological Society of America Bulletin* **121**, 1611-1628

HOLFORD, S.P., GREEN, P.F., HILLIS, R.R., UNDERHILL, J.R., STOKER, M.S., DUDDY, I.R., 2010. Multiple post-Caledonian exhumation episodes across NW Scotland revealed by apatite fission-track analysis. *Journal of the Geological Society* **167**, 675-694.

JAPSEN, P., CHALMERS, J.A., 2000. Neogene uplift and tectonics around the North Atlantic: overview. *Global and Planetary Change* **24**, 165-173.

JAPSEN, P., CHALMERS, J.A., GREEN, P.F., BONOW, J.M., 2011. Elevated, passive conrtinental margins: not rift shoulders, but expressions of episodic, post-rift burial and exhumation. *Global and Planetary Change* **90-91**, 73-86.

JONES, S.M., WHITE, N., LOVELL, B., 2001. Cenozoic and Cretaceous transient uplift in the Porcupine Basin and its relationship to a mantle plume, in: Shannon, P.M., Haugton, P.D., Corcoran, D.V. (Eds.), *The petroleum exploration of Ireland's offshore bassins. Geological Society, London, Special Publications* **188**, 345-360.

JONES, S., WHITE, N., CLARKE, B.J., ROWLEY, E., GALLAGHER, K., 2002. Present and past influence of the Iceland Plume on sedimentation, in: Doré, A.G., Cartwright, M.S., Stoker, M.S., Turner, J.P., White, N. (Eds.), *Exhumation of the North Atlantic margin: timing, mechanisms and implications for the petroleum exploration. Geological Society, London, Special Publications*, **196**, 13-25.

KEELEY, M.L., LEWIS, C.L.E., SEVASTOPULO, G.D., CLAYTON, G., BLACKMORE, R., 1993. Apatite fission track data from southeast Ireland: implications for post-Variscan

673 burial history. *Geological Magazine* **130**, 171-176.

674 KETCHAM, R.A., CARTER, A., DONELICK, R.A., BARBARAND, J., HURFORD, A.J.,
675 2007. Improved modeling of fission-track annealing in apatite. *American Mineralogist*
676 **92**, 799-810.

677 MASSON, D.G., MONTADERT, L., SCRUTTON, R.A., 1984. Regional geology of the
678 Goban Spur Continental Margin, in: De Graciansky, P.C., Poag, C.W., al., e. (Eds.).
679 *Initial Reports of the Deep Sea Drilling Project. US Government Printing Office,*
680 *Washington, D.C.* **80**. 1115 - 1139.

681 MCCULLOCH, A.A., 1993. Apatite fission track results from Ireland and the
682 Porcupine basin and their significance for the evolution of the North Atlantic. *Marine*
683 *and Petroleum Geology* **10**, 572-590.

684 MCCULLOCH, A.A., 1994. Low temperature thermal history of eastern Ireland:
685 effects of fluid flow. *Marine and Petroleum Geology* **11**, 389-399.

686 MCDONNELL, A., SHANNON, P.M., 2001. Comparative Tertiary stratigraphic
687 evolution of the Porcupine and Rockall basins. *The petroleum exploration of Ireland's*
688 *offshore bassins. Geological Society, London, Special Publications* **188**, 323-344.

689 MEESTERS, A.G.C.A., DUNAI, T.J., 2002. Solving the production-diffusion
690 equation for finite diffusion domains of various shapes: Part II. Application to cases
691 with [alpha]-ejection and nonhomogeneous distribution of the source. *Chemical*
692 *Geology* **186**, 57-73.

693 MOORE, J.G., 1992. A syn-rift to post-rift transition sequence in the Main
694 Porcupine Basin, offshore western Ireland, in: Parnell, J. (Eds.), *Basins on the*
695 *Atlantic seaboard: petroleum geology, sedimentology and basin evolution*. *Geological*
696 *Society, London, Special Publications* **62**, 333-349.

697 NAYLOR, D., 1992. The post-Variscan history of Ireland, in: Parnell, J. (Eds.),
698 *Basins on the Atlantic seaboard: petroleum geology, sedimentology and basin*
699 *evolution Geological Society, London, Special Publications* **62**, 255-275.

700 NAYLOR, D., 1998. Irish shoreline through geological time. *John Jackson*
701 *lectures. Occasional papers in Irish science and technology* **17**. Royal Dublin Society.

702 NAYLOR, D., SHANNON, P.M., 2005. The structural framework of the Irish Atlantic
703 Margin. *Geological Society, London, Petroleum Geology Conference series* **6**, 1009-

1021.

NAYLOR, D., SHANNON, P.M., 2009. Geology of Offshore Ireland, in: Holland, C.H., Sander, I.S. (Eds.), *The geology of Ireland, 2nd edition*. Dunedin Academic Press ltd, Edinburgh, Scotland, pp. 405-460.

O'CONNOR, P.J., LONG, C.B., BASHAM, I.R., SWAINBANK, I.G., BEDDOESTEPHENS, B., 1984. Age and geological setting of Uranium mineralization associated with the main Donegal granite, Ireland. *Transactions of the Institution of Mining and Metallurgy: Section B-Applied Earth Science* **93**, B190-B194.

PERSANO, C., BARFOD, D.N., STUART, F.M., BISHOP, P., 2007. Constraints on early Cenozoic underplating-driven uplift and denudation of western Scotland from low temperature thermochronometry. *Earth and Planetary Science Letters* **263**, 404-419.

REDFIELD, T.F., 2010. On apatite fission track dating and the Tertiary evolution of West Greenland topography. *Journal of the Geological Society* **167**, 261-271.

SAMBRIDGE, M., GALLAGHER, K., JACKSON, A., RICKWOOD, P., 2006. Trans-dimensional inverse problems, model comparison and the evidence. *Geophysical Journal International* **167**, 528-542.

SEILER, C., FLETCHER, J.M., KOHN, B.P., GLEADOW, A.J.W., RAZA, A., 2011. Low-temperature thermochronology of northern Baja California, Mexico: Decoupled slip-exhumation gradients and delayed onset of oblique rifting across the Gulf of California. *Tectonics* **30**, TC3004.

SHANNON, P.M., 1991. The development of Irish offshore sedimentary basins. *Journal of the Geological Society* **148**, 181-189.

SHANNON, P.M., MOORE, J.G., JACOB, A.W.B., MAKRIS, J., 1993. Cretaceous and Tertiary basin development west of Ireland. *Geological Society, London, Petroleum Geology Conference series* **4**, 1057-1066.

SHANNON, P.M., JACOB, A.W.B., O'REILLY, B.M., HAUSERR, F., READMAN, P.W., MAKRIS, J., 1999. Structural setting, geological development and basin modelling in the Rockall Trough. *Geological Society, London, Petroleum Geology Conference series* **5**, 421-431.

SHUSTER, D.L., FARLEY, K.A., 2009. The influence of artificial radiation damage

735 and thermal annealing on helium diffusion kinetics in apatite. *Geochimica et*
736 *Cosmochimica Acta* **73**, 183-196.

737 SIMMS, M.J., BOULTER, M.C., 2000. Oligocene cave sediments in Co. Cork:
738 implications for reconstructing the Tertiary landscape of southwest Ireland.
739 *Proceedings of the Geologists' Association* **111**, 363-372.

740 STOKER, M.S., PRAEG, D., SHANNON, P.M., HJELSTUEN, B.O., LABERG, J.S.,
741 NIELSEN, T., VAN WEERING, T.C.E., SEJRUP, H.P., EVANS, D., 2005. Neogene evolution
742 of the Atlantic continental margin of NW Europe (Lofoten Islands to SW Ireland):
743 anything but passive. *Geological Society, London, Petroleum Geology Conference*
744 *series* **6**, 1057-1076.

745 THOMPSON, P., 1985. *Dating the British Tertiary Igneous Province in Ireland by*
746 *the 40Ar–39Ar stepwise degassing method*. Unpublished thesis, University of
747 Liverpool.

748 UNDERHILL, J.R., PARTINGTON, M.A., 1993. Jurassic thermal doming and
749 deflation in the North Sea: implications of the sequence stratigraphic evidence.
750 *Geological Society, London, Petroleum Geology Conference series* **4**, 337-345.

751 WATTS, W.A., 1957. A Tertiary deposit in County Tipperary. *The scientific*
752 *proceedings of the Royal Dublin Society* **27**, 308-311.

753 WHITE, N., LOVELL, B., 1997. Measuring the pulse of a plume with the
754 sedimentary record. *Nature* **387**, 888-891.

755

756 **Figure captions**

757

758 Figure 1: Geological map of western Ireland showing the samples locations and key
759 localities discussed in the text.

760

761 Figure 2: Map of the Irish Atlantic margin modified from Naylor and Shannon (2009).
762 The onshore topogography employs the SRTM, 3 arc-second (ca. 90 m) dataset. Ca:

763 Carrauntoohill; Ba: Ballydeenlea; Mb: Mount Brandon; Mw: Mweelrea; Sl: Slieve
764 Snaght.
765
766 Figure 3: (a) Relationship between AFT age and mean track length (MTL), also
767 termed a boomerang plot for our dataset and previously published data. (b) Plot of
768 AFT age vs. elevation.
769
770 Figure 4: (a) Plot of F_T-corrected (U+Th)/He age *vs* AFT age (eU). The dashed
771 diagonal line corresponds to the line of equal AHe and AFT age. (b) Plot of F_T-
772 corrected (U-Th)/He age vs effective uranium content (eU).
773
774 Figure 5: Graphs of the thermal histories inferred from the inverse modelling of the
775 different profiles. For each thermal history model, the thick dark blue line is the
776 coolest (highest elevation sample) of the profile, with its credible interval denoted by
777 thin blue lines. The thick red line is the hottest (lowest elevation sample) of the
778 profile, with its credible interval denoted by thin purple lines. The grey lines are the
779 intermediate samples and the dashed horizontal lines are the temperature limits of
780 the PAZ. The black boxes are user-specified temperature-time constraints. (a) Slieve
781 Snaght profile; (b) Mweelrea profile; (c) Mount Brandon profile; (d) Ballydeenlea
782 sample and (e) Carrauntoohill profile.
783
784 Figure 6: Graphs of AFT and AHe age predicted for each model depicted in Fig. 5 vs
785 observed ages. The dashed diagonal line corresponds to a perfect fit of the predicted
786 age *vs* model age.
787

Figure 7: Predicted (red curves with credible intervals denoted by thin grey lines) and observed (blue histogram boxes) track length distributions for the thermal history models depicted in Fig. 5.

Figure 8: Thermal history model and predicted ages and track length distributions for the Mount Brandon profile with user-specified constraints to force an Early Cenozoic exhumation event. Colours are the same as in Figure 5.

Figure 9: Schematic geological evolution of the Irish Atlantic margin. During the Mesozoic, uplift and erosion of the rift shoulder flanks induces the first phase of exhumation (ca. 2.5 km) that cooled the samples to surface temperatures. Following exhumation, there was deposition of a thick sedimentary sequence that resulted in ca. 1.5 km of burial. A phase of Palaeocene exhumation may have occurred prior to a final Neogene pulse of exhumation that brought the samples to the surface. See text for discussion.

Table 1: Fission track results.

[1]Coordinates are for the Irish National Grid system.

[2]Number of spontaneous tracks.

[3]Sum of the individual grain $^{238}U/^{43}Ca$ ratios measured by ICPMS and weighted by the counted area.

[4]Counted area.

For the Slieve Snaght profile, the weighted mean U-Pb age is pooled from all samples.

813 Table 2: (U-Th/He) results

814 [1] (2) following the aliquot number indicates that two grains were picked for these
815 aliquots.

816

FIGURE 1

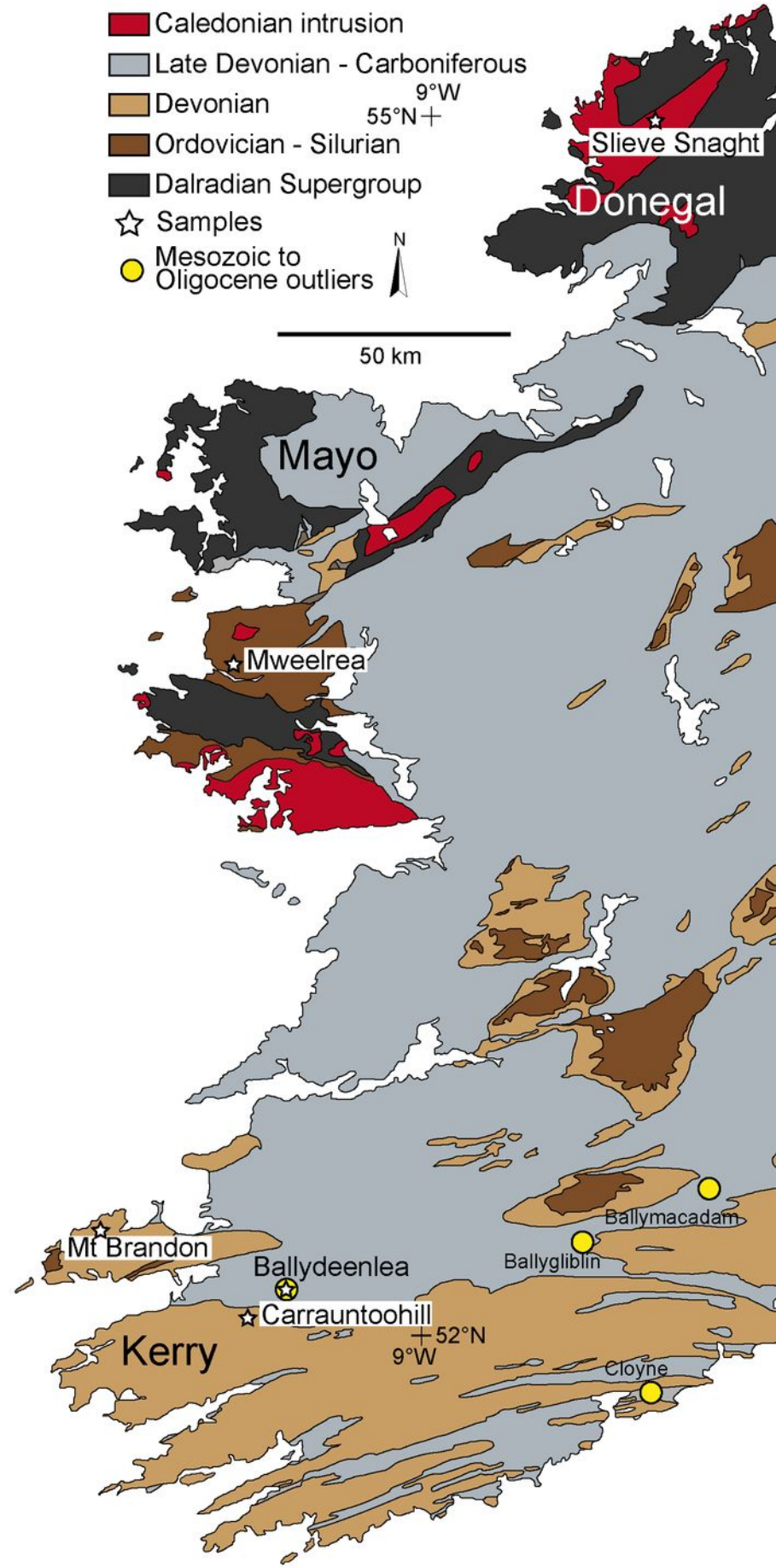
Caledonian intrusion
Late Devonian - Carboniferous
Devonian
Ordovician - Silurian
Dalradian Supergroup
Samples
Mesozoic to Oligocene outliers
9°W
55°N
N
50 km
Slieve Snaght
Donegal
Mayo
Mweelrea
Ballymacadam
Ballygliblin
Mt Brandon
Ballydeenlea
Carrauntoohill
Kerry
52°N
9°W
Cloyne

FIGURE 2

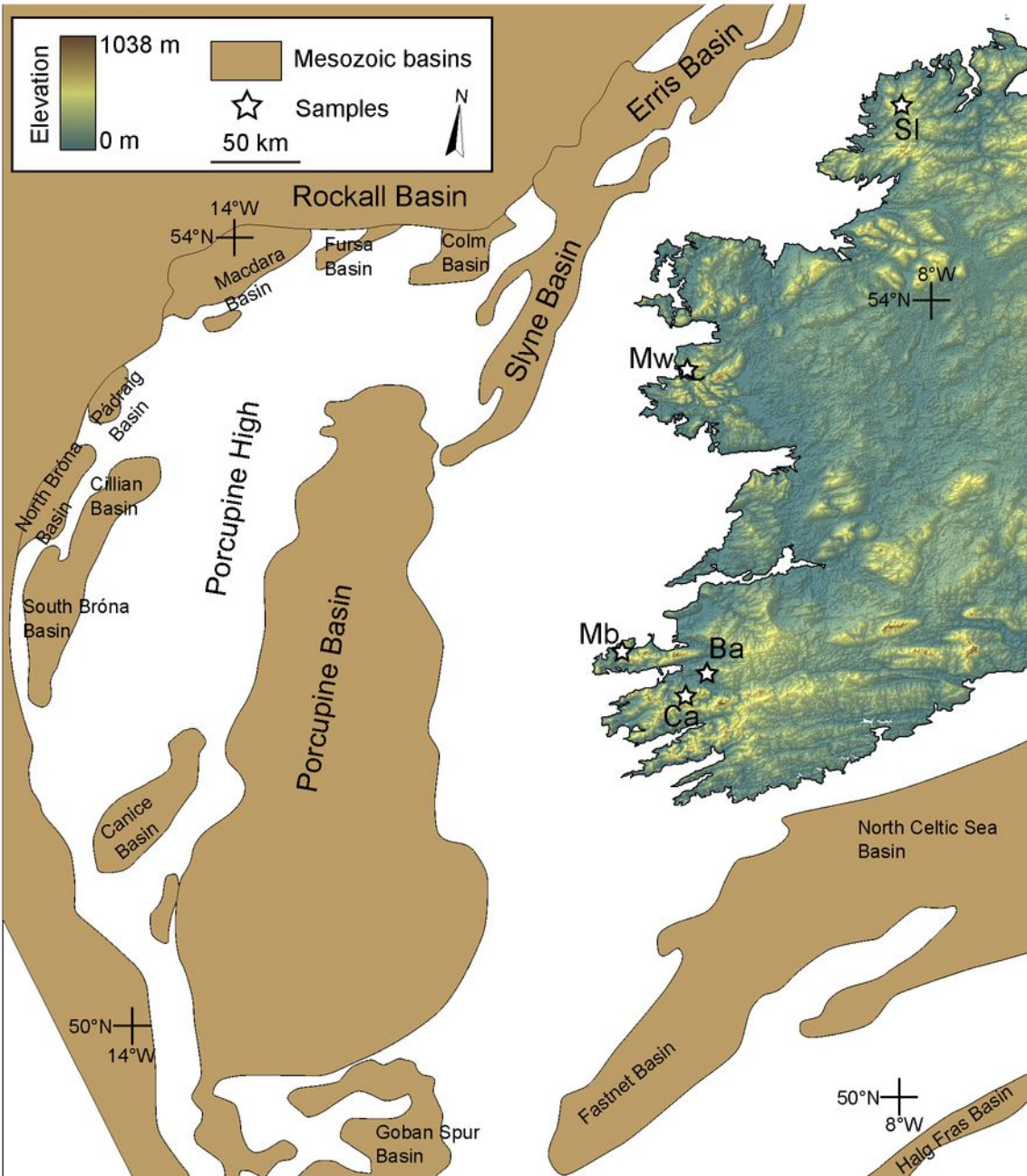
Elevation
1038 m
0 m
Mesozoic basins
Samples
50 km
N
Erris Basin
Rockall Basin
14°W
54°N
Macdara Basin
Fursa Basin
Colm Basin
Slyne Basin
Padraig Basin
North Bróna Basin
Cillian Basin
Porcupine High
Porcupine Basin
South Bróna Basin
Canice Basin
50°N
14°W
Goban Spur Basin
Sl
8°W
54°N
Mw
Mb
Ba
Ca
North Celtic Sea Basin
Fastnet Basin
50°N
8°W
Halg Fras Basin

FIGURE 3

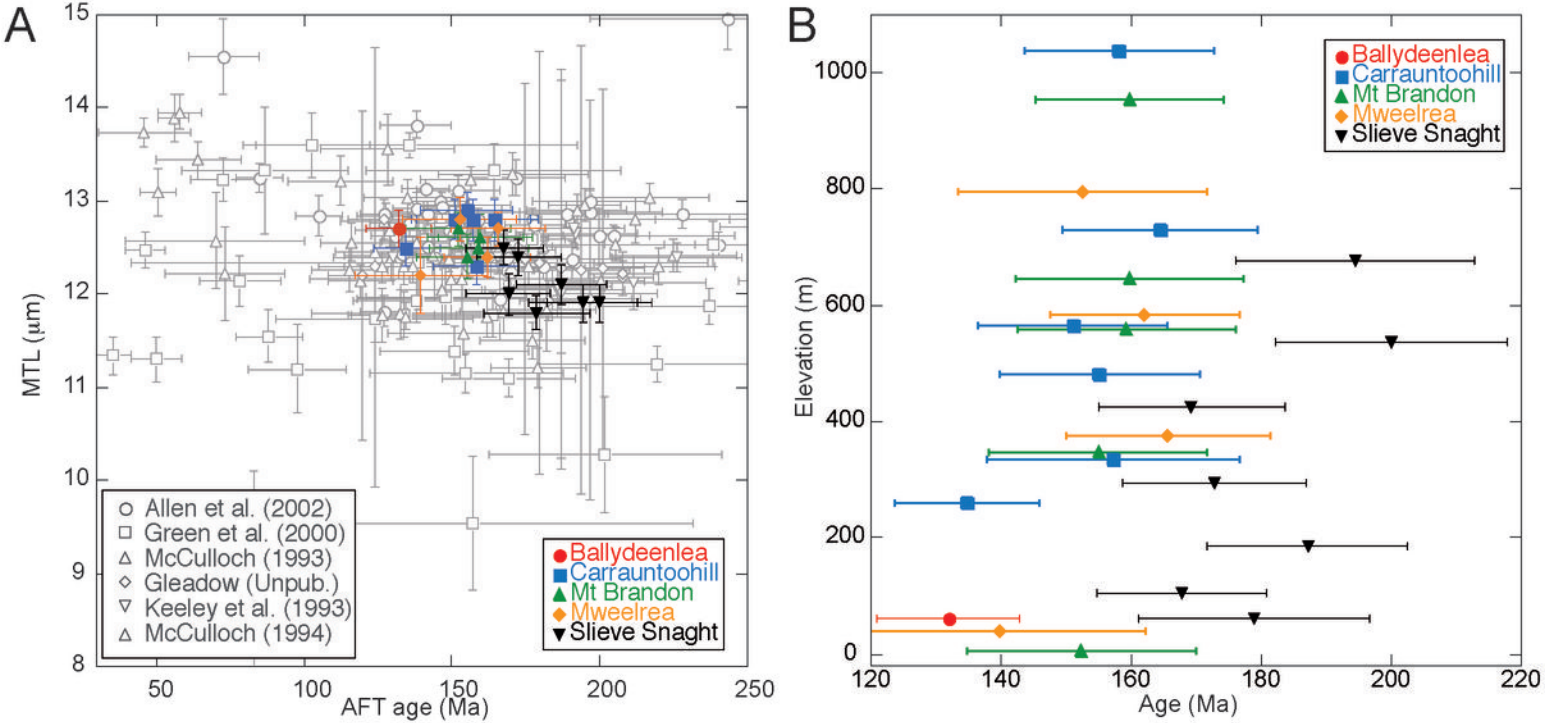
A
MTL (μm)
AFT age (Ma)
Allen et al. (2002)
Green et al. (2000)
McCulloch (1993)
Gleadow (Unpub.)
Keeley et al. (1993)
McCulloch (1994)
Ballydeenlea
Carrauntoohill
Mt Brandon
Mweelrea
Slieve Snaght
B
Elevation (m)
Age (Ma)
Ballydeenlea
Carrauntoohill
Mt Brandon
Mweelrea
Slieve Snaght

FIGURE 4

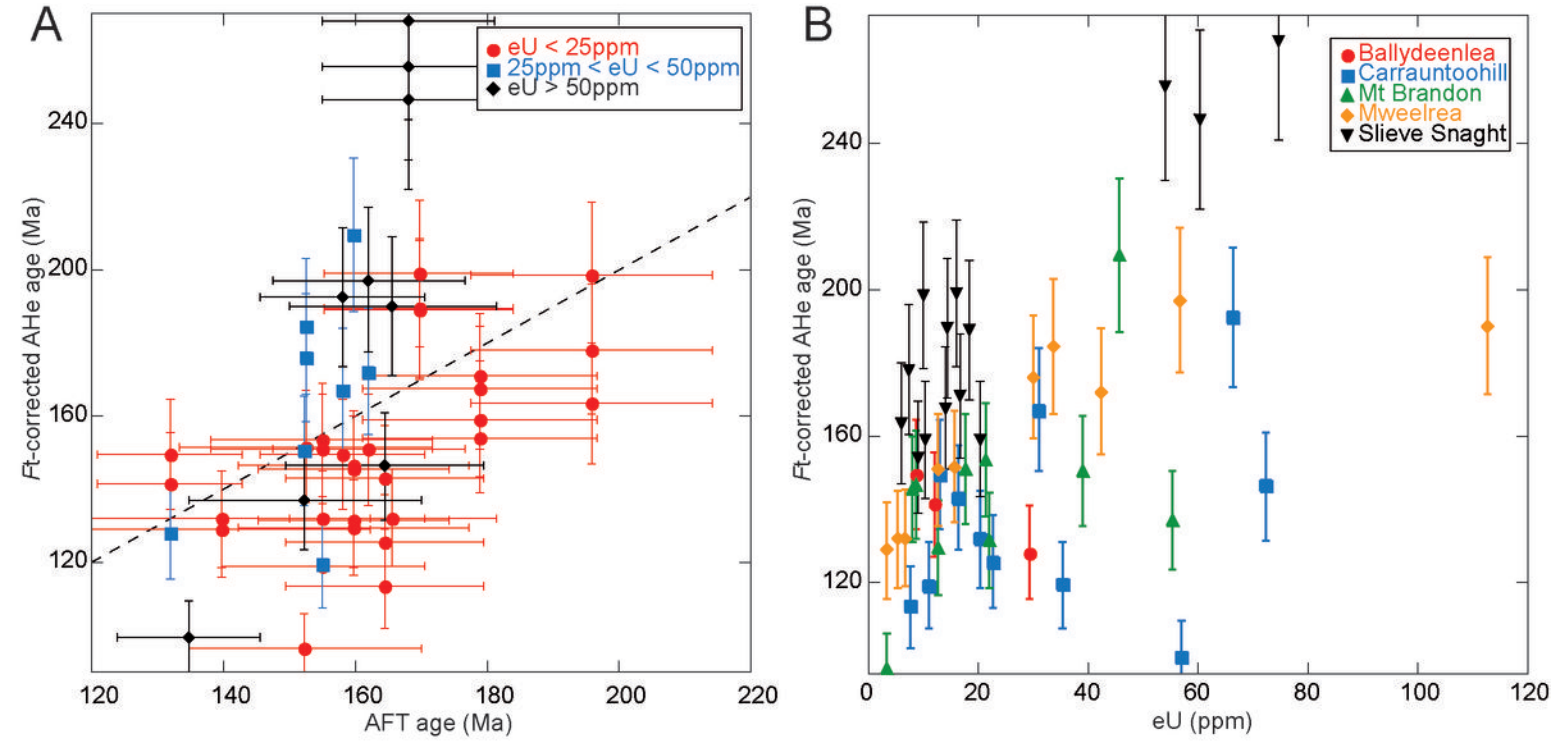
A
eU < 25ppm
25ppm < eU < 50ppm
eU > 50ppm
240
200
160
120
Ft-corrected AHe age (Ma)
120
140
160
180
200
220
AFT age (Ma)
B
Ballydeenlea
Carrauntoohill
Mt Brandon
Mweelrea
Slieve Snaght
240
200
160
120
Ft-corrected AHe age (Ma)
0
20
40
60
80
100
120
eU (ppm)

FIGURE 5

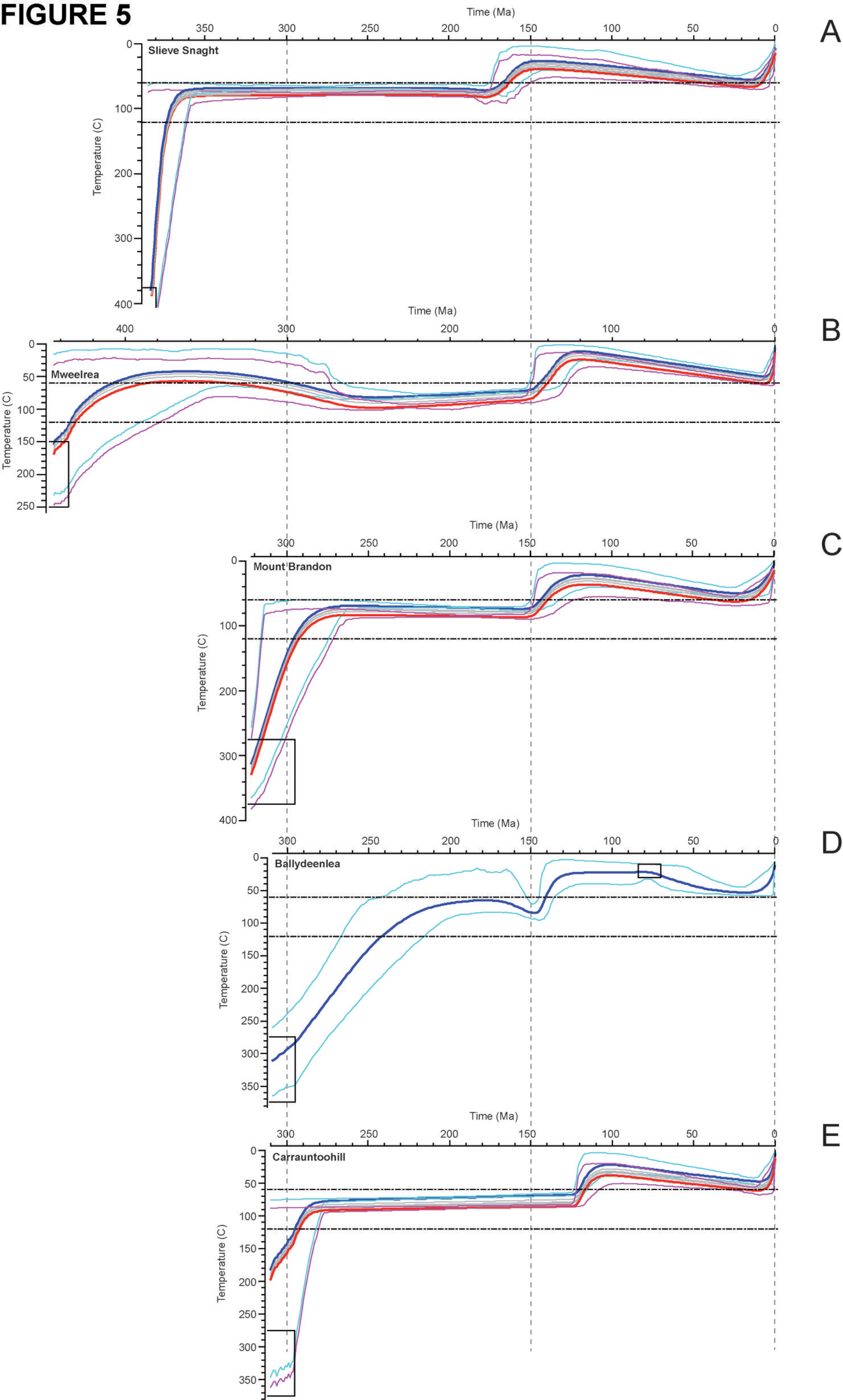
A
Time (Ma)
350
300
250
200
150
100
50
0
Slieve Snaght
Temperature (C)
0
100
200
300
400
B
Time (Ma)
400
300
200
100
0
Mweelrea
Temperature (C)
0
50
100
150
200
250
C
Time (Ma)
300
250
200
150
100
50
0
Mount Brandon
Temperature (C)
0
100
200
300
400
D
Time (Ma)
300
250
200
150
100
50
0
Ballydeenlea
Temperature (C)
0
50
100
150
200
250
300
350
E
Time (Ma)
300
250
200
150
100
50
0
Carrauntoohill
Temperature (C)
0
50
100
150
200
250
300
350

FIGURE 6

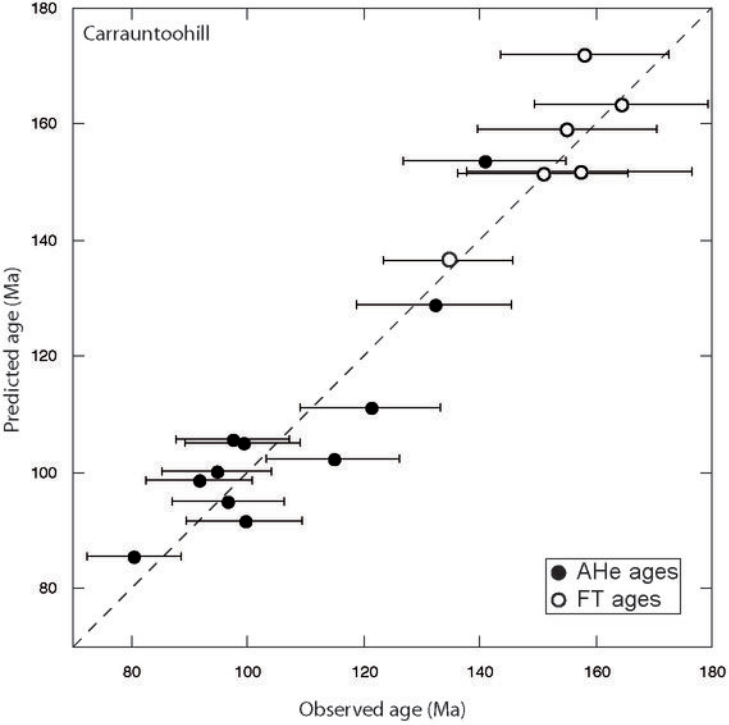
Carrauntoohill
Predicted age (Ma)
Observed age (Ma)
AHe ages
FT ages

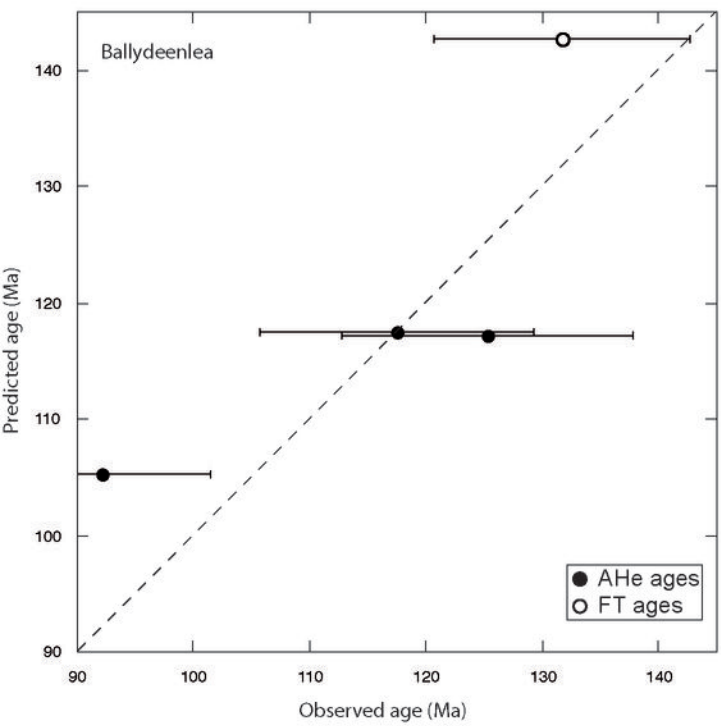
Ballydeenlea
Predicted age (Ma)
Observed age (Ma)
AHe ages
FT ages

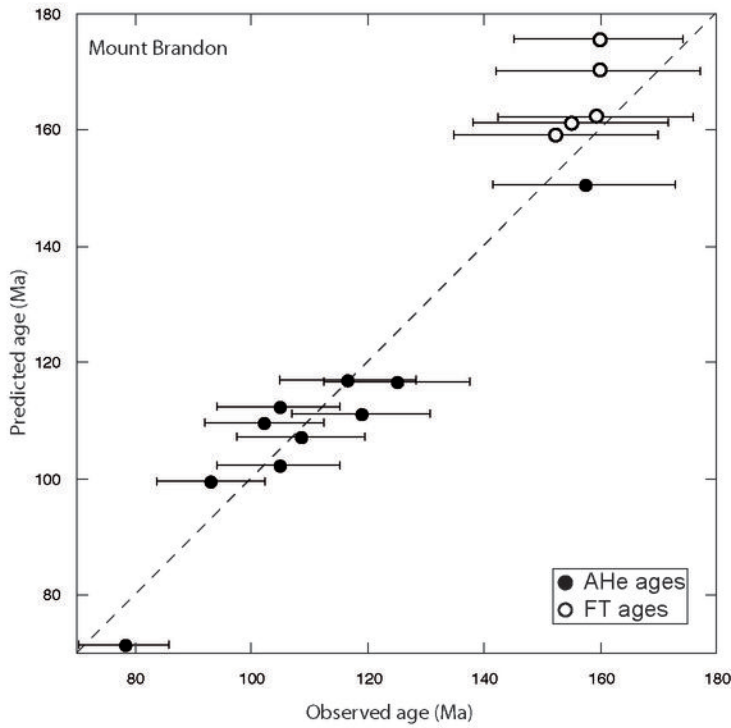
Mount Brandon
Predicted age (Ma)
Observed age (Ma)
AHe ages
FT ages

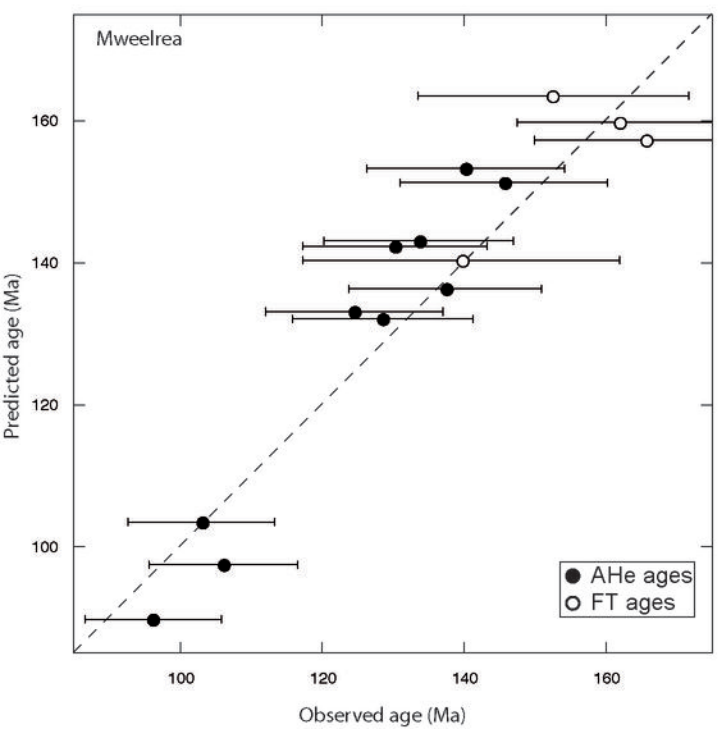
Mweelrea
Predicted age (Ma)
Observed age (Ma)
AHe ages
FT ages

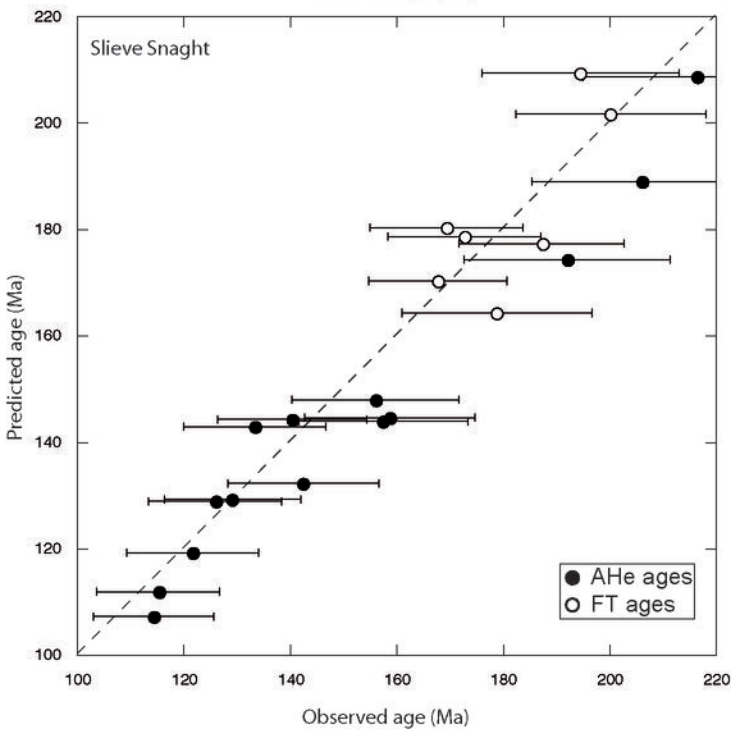
Slieve Snaght
Predicted age (Ma)
Observed age (Ma)
AHe ages
FT ages

FIGURE 7

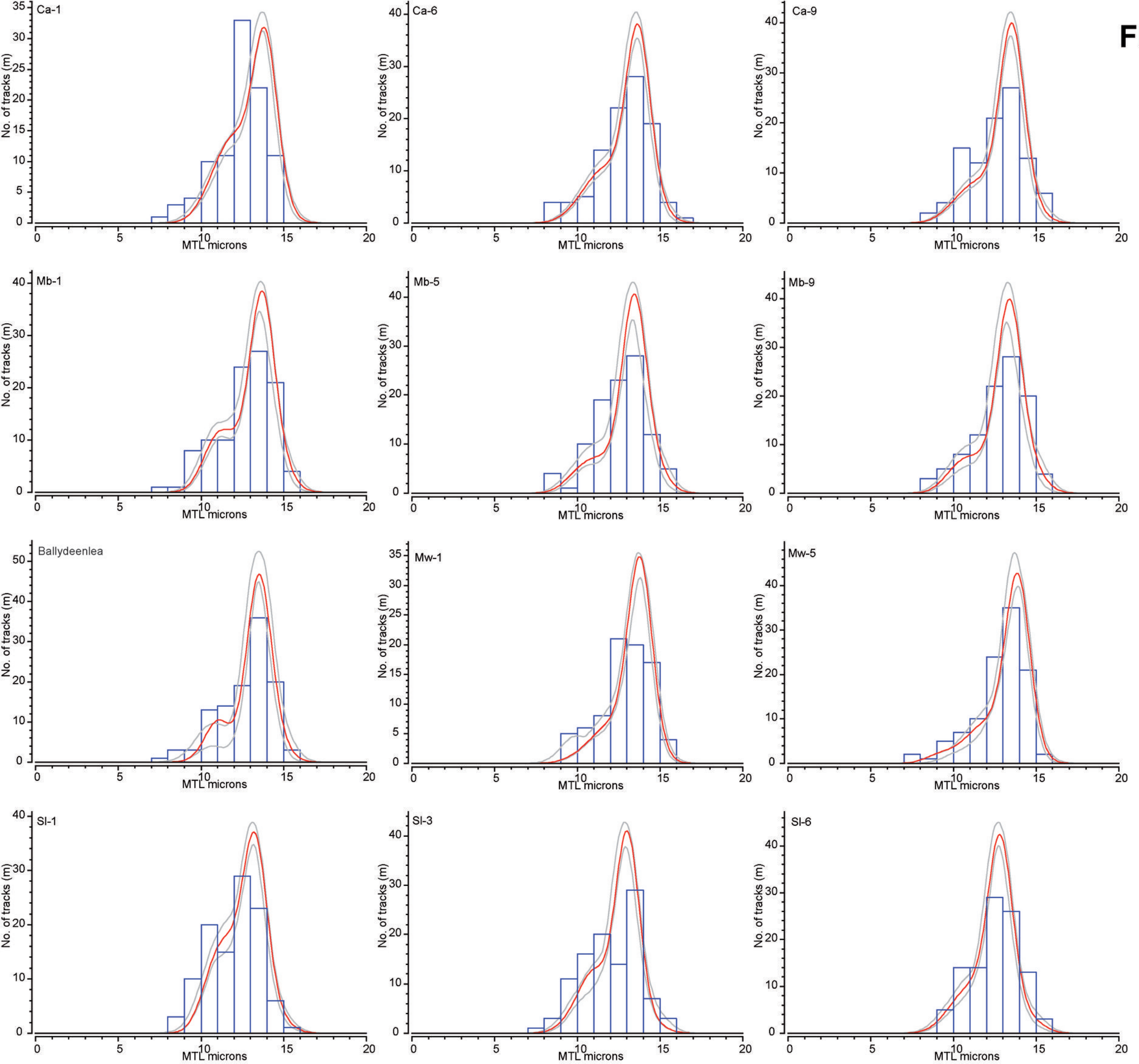
Ca-1
Ca-6
Ca-9
Mb-1
Mb-5
Mb-9
Ballydeenlea
Mw-1
Mw-5
Sl-1
Sl-3
Sl-6
No. of tracks (m)
MTL microns

FIGURE 8

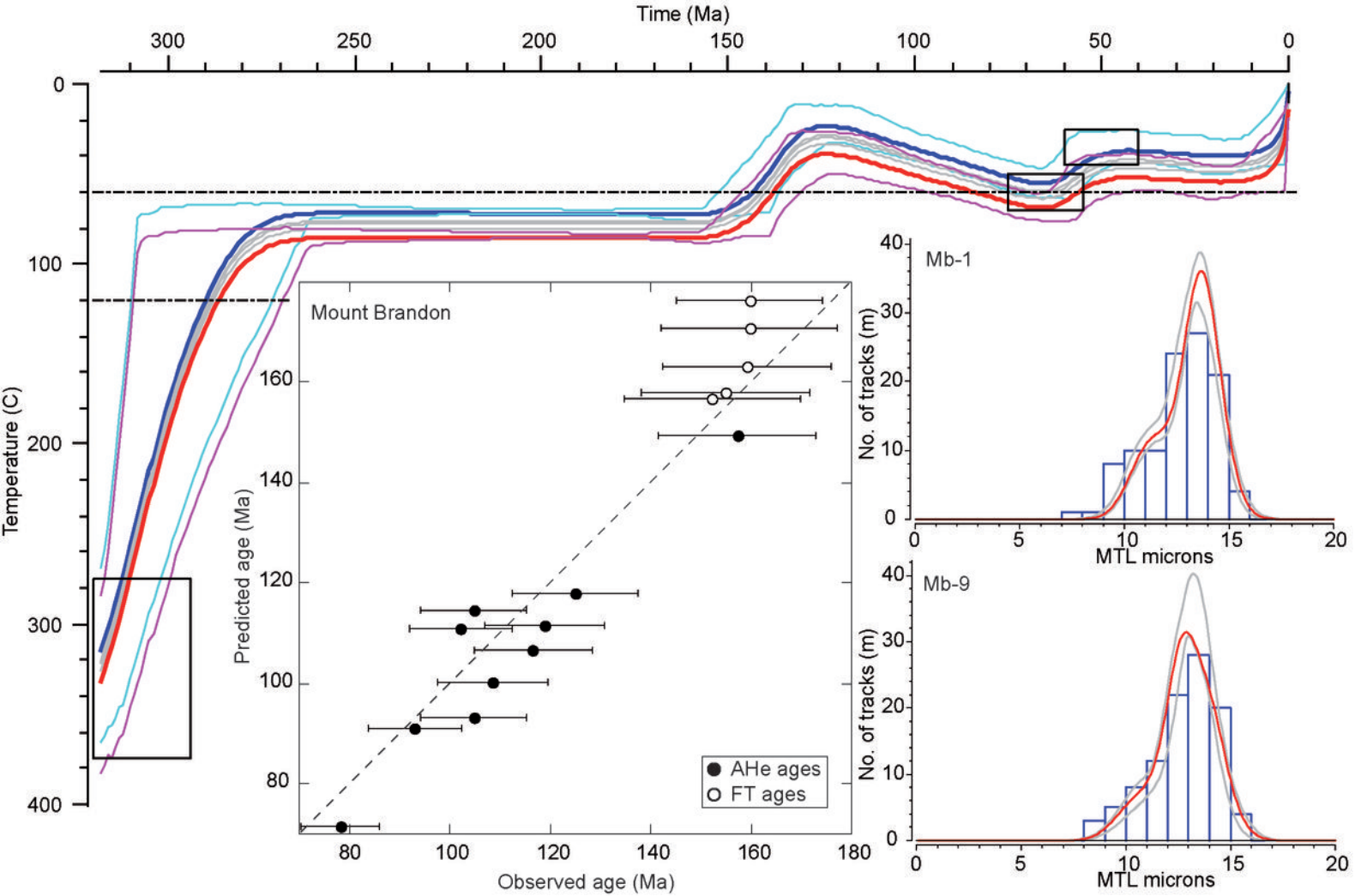
Time (Ma)
300
250
200
150
100
50
0
Temperature (C)
0
100
200
300
400
Mount Brandon
Predicted age (Ma)
Observed age (Ma)
80
100
120
140
160
180
AHe ages
FT ages
Mb-1
No. of tracks (m)
MTL microns
Mb-9
No. of tracks (m)
MTL microns

FIGURE 9

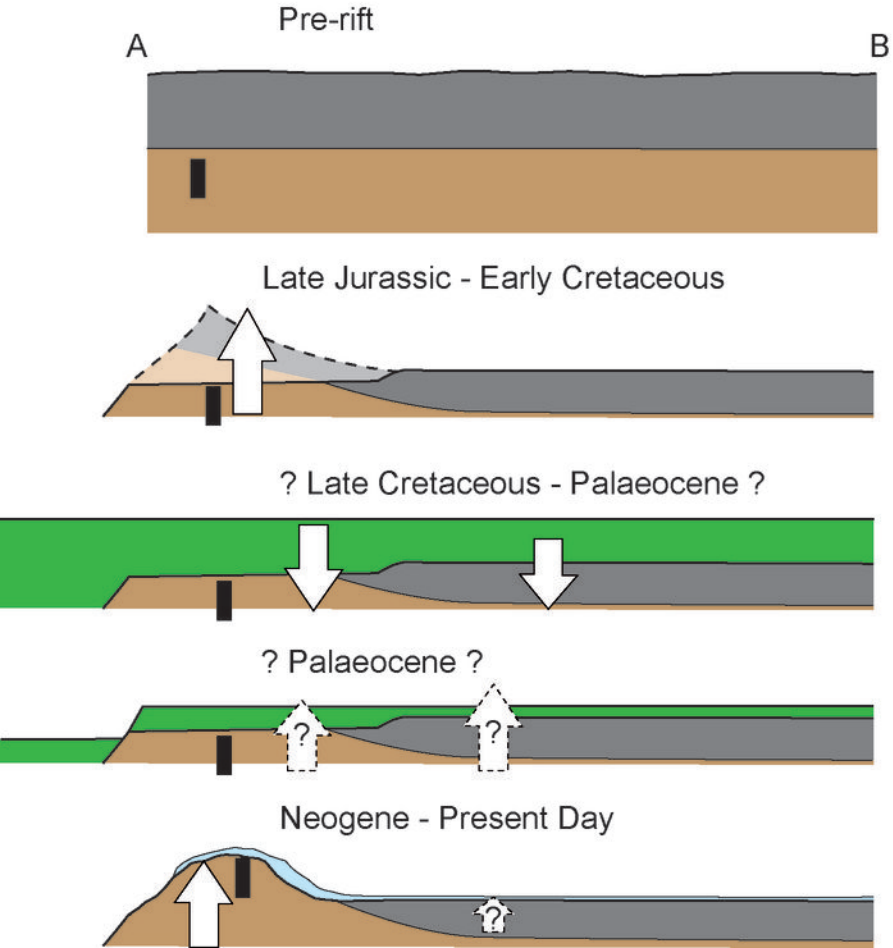

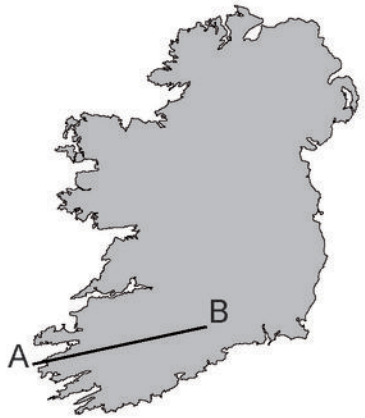

(*) Devonian Old Red Sandstone
(*) Eroded during Mesozoic rifting

(*) Carboniferous sediments
(*) Eroded during Mesozoic rifting

Late Cretaceous - ? Palaeogene ? sediments now eroded

Pleistocene ice sheet

Phase of exhumation / burial

Sample profile

TABLE 1

Name	Stratigraphic / Emplacement Age	Easting[1]	Northing	Elevation	Ns [2]	$^{238}U/^{43}Ca$ [3]	Area (cm^2) [4]	FT Age (Ma)
Ballydeenlea								
Ba-B2	Campanian	95300	97700	60	663	4.95E-05	6.14E-04	131.8
Carrauntoohill								
Ca-1	Middle Devonian	80366	84417	1038	587	3.66E-05	3.75E-04	158.1
Ca-4	Middle Devonian	80702	83669	731	610	3.61E-05	5.27E-04	164.4
Ca-6	Middle Devonian	80895	83776	566	532	3.44E-05	4.11E-04	151
Ca-7	Middle Devonian	81054	83873	480	499	3.15E-05	3.91E-04	155.1
Ca-8	Middle Devonian	81666	84498	334	499	3.11E-05	3.59E-04	157.3
Ca-9	Middle Devonian	82227	85829	259	787	5.73E-05	6.35E-04	134.7
Mount Brandon								
Mb-1	Lower Devonian	46035	111628	953	617	3.79E-05	4.38E-04	159.7
Mb-4	Lower Devonian	45383	110953	645	395	2.41E-05	4.76E-04	159.7
Mb-5	Lower Devonian	45075	110678	558	418	2.58E-05	3.59E-04	159.2
Mb-7	Lower Devonian	44301	109383	348	399	2.51E-05	3.87E-04	155
Mb-9	Lower Devonian	42335	112043	5	353	2.24E-05	4.61E-04	152.3
Mweelrea								
Mw-1	Upper Ordovician	80251	268295	795	279	1.80E-05	3.09E-04	152.6
Mw-3	Upper Ordovician	80905	267758	585	616	3.75E-05	3.28E-04	162
Mw-5	Upper Ordovician	81604	267634	374	549	3.25E-05	2.92E-04	165.7
Mw-8	Upper Ordovician	82803	269554	40	177	1.24E-05	4.46E-04	139.7
Slieve Snaght								
Sl-1	407±4 Ma	192364	414816	678	570	2.84E-05	4.19E-04	194.5

Sl-2	407±4 Ma	192800	414683	537	644	3.14E-05	4.22E-04	200.1
Sl-3	407±4 Ma	192933	413863	425	722	4.16E-05	3.06E-04	169.3
Sl-4	407±4 Ma	192848	413616	294	802	4.55E-05	2.79E-04	172.7
Sl-5	407±4 Ma	193137	413176	185	790	4.11E-05	2.79E-04	187.2
Sl-6	407±4 Ma	193421	412909	104	940	5.47E-05	2.90E-04	167.8
Sl-7	407±4 Ma	191011	410249	65	485	2.65E-05	3.22E-04	178.8

± 2s (Ma)	# grains	P(c^2)	MTL (μm)	SE (μm)	SD (μm)	# tracks	Dpar (μm)	Cl wt%	U-Pb age (Ma)
11.0	21	0.06	12.7	0.21	2.23	112	1.65	0.09	417.0
14.6	20	<0.05	12.3	0.19	1.87	95	1.52	0.07	419.0
15.0	23	0.21	12.8	0.22	2.15	95	1.72	0.06	403.0
14.6	20	0.28	12.8	0.21	2.12	101	1.66	0.15	406.0
15.4	20	0.11	12.9	0.19	1.90	102	2.08	0.08	416.0
19.4	20	0.11	12.8	0.22	2.08	91	1.63	0.08	425.0
11.2	20	0.10	12.5	0.21	2.09	100	1.60	0.09	410.0
14.4	22	0.63	12.6	0.20	2.07	106	1.49	0.11	412.0
17.6	19	0.12	12.6	0.26	1.94	54	1.49	0.14	426.0
16.8	19	0.09	12.5	0.20	2.01	102	1.59	0.06	423.0
16.8	22	0.39	12.4	0.24	2.23	85	1.60	0.04	420.0
17.6	20	0.07	12.7	0.19	1.97	102	1.50	0.06	416.0
19.2	20	0.10	12.8	0.23	2.09	81	1.63	0.08	454.0
14.6	23	0.28	12.4	0.21	2.11	102	1.60	0.09	443.5
15.6	21	0.25	12.7	0.19	2.00	107	1.61	0.04	446.3
22.4	20	0.05	12.2	0.41	2.13	27	1.78	0.15	453.0
18.4	23	0.05	11.9	0.20	2.11	107	1.44	0.02	

17.8	23	0.09	11.9	0.21	2.16	104	1.41	0.03	
14.4	20	0.05	12.0	0.23	2.33	104	1.47	0.02	
14.2	21	0.32	12.4	0.19	1.91	103	1.49	0.07	
15.4	20	0.10	12.1	0.21	2.16	101	1.41	0.04	
13.0	19	0.07	12.5	0.19	1.95	104	1.45	0.07	(weighted ave
17.8	16	0.06	11.8	0.19	1.94	101	1.30	0.02	384.0

± 2s (Ma)	MSWD
15.0	3.3
16.0	5.6
16.0	3.2
15.0	6.4
16.0	3.9
16.0	4.2
19.0	7.9
11.0	2.2
32.0	3.0
15.0	1.9
16.0	2.8
21.0	3.2
34.0	7.8
9.5	3.1
8.8	3.0
23.0	2.9

rage of all 7 samples)

2.9	2.9

TABLE 2

Sample[1]	U(ppm)	Th(ppm)	Eu (ppm)	Th/U	He (nmol/g)	Age (Ma)	± 1s Ma	*F*t
BA-B2								
-2	5.62	13.08	8.76	2.33	5.97E-06	125.3	12.5	0.838
-3	8.84	13.45	12.07	1.52	7.73E-06	117.5	11.8	0.832
-5	28.02	5.50	29.34	0.20	1.48E-05	92.2	9.2	0.719
Ca-1								
-2	11.80	4.45	12.87	0.38	8.10E-06	114.8	11.5	0.768
-4 (2)	23.30	31.65	30.90	1.36	2.23E-05	132.2	13.2	0.791
-5 (2)	36.18	125.24	66.24	3.46	5.07E-05	140.9	14.1	0.732
Ca-4								
-1	10.40	50.88	22.61	4.89	1.21E-05	99.3	9.9	0.79
-2	3.65	16.84	7.69	4.61	3.95E-06	94.8	9.5	0.837
-4	13.85	10.20	16.30	0.74	1.08E-05	121.3	12.1	0.847
-5 (2)	35.78	152.90	72.48	4.27	3.83E-05	97.6	9.8	0.667
Ca-7								
-1	29.51	24.97	35.50	0.85	1.77E-05	91.6	9.2	0.768
-3	13.24	29.72	20.37	2.24	1.04E-05	99.5	9.9	0.754
-4	0.01	46.02	11.05	-	5.72E-06	96.7	9.7	0.811
Ca-9								
-5	46.78	43.02	57.10	0.92	2.50E-05	80.5	8.1	0.808
Mb-1								
-2	36.21	39.65	45.73	1.10	3.94E-05	157.3	15.7	0.751
-3	5.02	70.41	21.92	14.03	1.24E-05	104.8	10.5	0.797
-5	5.89	9.22	8.10	1.57	6.57E-06	108.5	10.9	0.745
Mb-4								
-2	6.88	7.91	8.78	1.15	5.58E-06	116.6	11.7	0.795

-4	11.10	6.91	12.76	0.62	6.49E-06	93.0	9.3	0.718
Mb-7								
-2	17.22	2.52	17.82	0.15	1.02E-05	104.7	10.5	0.694
-3	16.41	20.81	21.40	1.27	1.39E-05	118.8	11.9	0.773
Mb-9								
-1	2.78	2.31	3.33	0.83	1.42E-06	78.2	7.8	0.811
-2	54.88	2.48	55.48	0.05	3.11E-05	102.2	10.2	0.746
-3	38.30	2.93	39.00	0.08	2.67E-05	124.9	12.5	0.829
Mw-1								
-1	28.37	6.55	29.94	0.23	2.75E-05	133.7	13.4	0.759
-3	9.61	25.00	15.61	2.60	1.06E-05	124.6	12.5	0.821
-4	33.02	3.19	33.79	0.10	2.55E-05	137.4	13.7	0.745
Mw-3								
-1	11.84	3.92	12.78	0.33	9.01E-06	128.5	12.8	0.852
-4	41.70	3.07	42.44	0.07	3.27E-05	140.3	14.0	0.815
-5	56.01	2.94	56.72	0.05	4.55E-05	145.7	14.6	0.739
Mw-5								
-3	101.10	47.74	112.56	0.47	8.03E-05	130.3	13.0	0.685
-4	5.23	6.16	6.71	1.18	3.53E-06	96.1	9.6	0.727
Mw-8								
-2	2.43	11.52	5.19	4.74	2.90E-06	102.9	10.3	0.781
-3	1.42	7.78	3.29	5.48	1.90E-06	106.0	10.6	0.823
Sl-1								
-1	10.11	5.64	11.47	0.56	1.00E-05	158.7	15.9	0.799
-4	7.32	0.70	7.49	0.10	5.02E-06	121.7	12.2	0.683
-5	6.05	1.95	6.52	0.32	4.51E-06	125.9	12.6	0.77
Sl-3								
-3	18.40	4.06	19.37	0.22	1.66E-05	156.0	15.6	0.825

-4	16.15	1.41	16.49	0.09	1.43E-05	157.5	15.8	0.792
-5	14.34	2.12	14.85	0.15	1.16E-05	142.4	14.2	0.752
Sl-6								
-2	74.69	2.80	75.36	0.04	9.04E-05	216.5	21.6	0.808
-3	54.18	13.71	57.47	0.25	6.54E-05	206.0	20.6	0.806
-5	60.19	4.98	61.39	0.08	6.51E-05	192.0	19.2	0.779
Sl-7								
-1	9.04	5.40	10.34	0.60	6.48E-06	114.4	11.4	0.742
-2	16.75	2.27	17.29	0.14	1.33E-05	140.3	14.0	0.82
-3	20.43	3.20	21.20	0.16	1.55E-05	133.4	13.3	0.838
-4	10.20	4.38	11.25	0.43	7.11E-06	115.3	11.5	0.725
-5	13.88	2.48	14.47	0.18	1.03E-05	129.1	12.9	0.77

Corrected age (Ma)	± 1s Ma
149.5	15.0
141.3	14.1
128.2	12.8
149.5	14.9
167.1	16.7
192.5	19.2
125.7	12.6
113.3	11.3
143.2	14.3
146.3	14.6
119.3	11.9
131.9	13.2
119.2	11.9
99.6	10.0
209.5	20.9
131.5	13.2
145.6	14.6
146.6	14.7

129.6	13.0
150.9	15.1
153.6	15.4
96.4	9.6
137.0	13.7
150.6	15.1
176.1	17.6
151.7	15.2
184.4	18.4
150.8	15.1
172.1	17.2
197.2	19.7
190.2	19.0
132.1	13.2
131.8	13.2
128.8	12.9
198.6	19.9
178.1	17.8
163.5	16.4
189.1	18.9

198.9	19.9
189.4	18.9
267.9	26.8
255.5	25.6
246.4	24.6
154.2	15.4
171.1	17.1
159.2	15.9
159.0	15.9
167.7	16.8